The Gross-Pitaevskii Equations and Beyond for Inhomogeneous Condensed Bosons

G. G. N. Angilella[1], S. Bartalini[2], F. S. Cataliotti[1,2,3], I. Herrera[1,2], N. H. March[4,5], R. Pucci[1]

[1]Dipartimento di Fisica e Astronomia, Università di Catania, and Lab. MATIS-INFM, and CNISM, UdR Catania, and INFN, Sez. Catania, Via S. Sofia, 64, I-95123 Catania, Italy.

[2]LENS, Dipartimento di Fisica, Università di Firenze, and Istituto Nazionale per la Fisica della Materia, UdR Firenze, Via Nello Carrara, 1, I-50019 Sesto Fiorentino (FI), Italy.

[3]Scuola Superiore di Catania, Università di Catania, Catania, Italy.

[4]Department of Physics, University of Antwerp, Groenenborgerlaan 171, B-2020 Antwerp, Belgium.

[5]Oxford University, Oxford, England.

Abstract

A simple derivation of the static Gross-Pitaevskii (GP) equation is given from an energy variational principle. The result is then generalized heuristically to the time-dependent GP form. With this as background, a number of different experimental areas explored very recently are reviewed, in each case contact being established between the measurements and the predictions of the GP equations. The various limitations of these equations as used on dilute inhomogeneous condensed Boson atomic gases are then summarized, reference also being made to the fact that there is no many-body wave function underlying the GP formulation. This then leads into a discussion of a recently proposed integral equation, derived by taking the Bogoliubov-de Gennes equation as starting point. Some limitations of the static GP differential equation are thereby removed, though it is a matter of further study to determine whether a correlated wave function exists as underpinning for the integral equation formulation.

1 Introduction

The purpose of this Chapter is to review recent progress in both theory and experiment in the area of inhomogeneous condensed bosons. Both statics and dynamics will be referred to in the course of this review. However, the field cited above is now vast, and therefore we shall select, in both experiment and theory, the areas in which our own contribution lie.

With the above brief outline, we next emphasize that, since the Gross-Pitaevskii (GP) equations, to be given explicitly in Section 2 below, have been very valuable in providing a theoretical framework, albeit quite approximate, for the interpretation of

an extensive body of experimental data, we shall take the GP equations as a focus for the present Chapter. However, to avoid repetition, we cite here two major reviews which should be consulted by the reader who requires more technical background to the basic theoretical arguments, and application techniques, underlying the GP equations.

The first of these is by Dalfovo *et al.* (1999). This provides an authorative review of the phenomenon of Bose-Einstein condensation (BEC) of dilute gases in harmonic traps from a theoretical perspective. For the ideal Bose gas, Dalfovo *et al.* treat *(i)* finite size effects, *(ii)* the role of dimensionality, and *(iii)* the thermodynamic limit of trapped Bosons at finite temperature. In addition, again for the ideal Bose gas, nonharmonic traps and adiabatic transformations are also treated. So in the present Chapter we shall take their treatment of the ideal Bose gas in traps as assumed background.

The second of the reviews referred to above is of very different character, but again provides invaluable background for this present Chapter. Thus the focus of the review by Minguzzi *et al.* (2004) is on numerical methods in use for atomic quantum gases with application to Bose-Einstein condensates, our dominant focus in this Chapter, but also Minguzzi *et al.* cover ultracold Fermions. Thus the reader interested specifically in numerical techniques used to solve practical problems in inhomogeneous assemblies of condensed Bosons should consult the extensive treatment of Minguzzi *et al.* (2004).

With this background, the outline of the present Chapter is as follows. In Section 2 both static and dynamic GP equations are set up by what we consider to be the simplest physical considerations. One example to illustrate the time-dependent GP Eq. (6) below, which will be summarized also in Section 2, is drop emission from an optical lattice under gravity (Anderson and Kasevich, 1998; Chiofalo *et al.*, 1999), while a somewhat generalized static GP equation is utilized in Fig. 1, which shows a vortex array for a rotating Bose-Einstein condensate. These two examples lead into Section 3, in which selected experiments are both described and also brought into contact with the GP equations. In particular, we shall focus on optical lattices, atom chips and magnetic microtraps, and the realization of Josephson Junction arrays of Bose-Einstein condensates (Cataliotti *et al.*, 2001). We will also briefly survey the dynamics of a BEC expanding in a moving 1D optical lattice, and some experiments beyond the GP equations. Section 4 is then a very brief discussion, following the arguments of Leggett (2003), of some limitations of the GP equations exposed by first-principles arguments. This leads into Sections 5 and 6, in which an integral equation transcending the static GP Eq. (4) is set up, following the proposal by Angilella *et al.* (2004). The Chapter concludes with a brief summary and some selected proposals for directions in which further studies should prove fruitful (Section 7).

2 Gross-Pitaevskii (GP) equations

The equations which provide a focus for the present review were proposed independently by Gross (1961, 1963) and by Pitaevskii (1961). However, it is fair to say that the mean-field description of a dilute Bose gas goes back at least to Bogoliubov (1947). The central point in his study was in separating out the condensate contribution. The generalization of the Bogoliubov approach to embrace the situations where there is both inhomogeneity and time-dependence is the aim of this section of the present review.

2.1 Static GP equation

The natural starting point then is to treat first the static, or time-independent case, for inhomogeneous condensed Bosons. This will lead to the so-called static GP equation. The approach we shall adopt below (see also Dalfovo *et al.*, 1999; Minguzzi *et al.*, 2004) is to start from variational minimization, for a Bose-condensed gas in a three-dimensional trap at zero temperature, of the energy functional $E[\Phi]$ given by

$$E[\Phi] = \int d\mathbf{r} \left[\frac{\hbar^2}{2m} |\nabla \Phi|^2 + V_{\rm ext}(\mathbf{r}) |\Phi|^2 + \frac{1}{2} g |\Phi|^4 \right]. \tag{1}$$

In this energy functional, $|\Phi(\mathbf{r})|^2$ is the inhomogeneous density profile, the so-called 'condensate wave function', $\Phi(\mathbf{r})$ playing the role of the order parameter of the Boson assembly. The first term on the right-hand-side (RHS) of Eq. (1) represents the kinetic energy of the condensate while the second is the potential energy due to the external confining potential $V_{\rm ext}(\mathbf{r})$. The final term on the RHS of Eq. (1) requires rather more discussion. It is appropriate in a dilute and cold gas as a representation of the atom-atom interaction, say in general $U(\mathbf{r} - \mathbf{r}')$, since in this case only binary collisions at low energy prove to have relevance. These collisions can be characterized, in fact, by a single parameter a, which denotes the s-wave scattering length, independently of the finer details of $U(\mathbf{r} - \mathbf{r}')$. As Dalfovo *et al.* (1999) stress, this permits one to adopt an effective interaction given by

$$U(\mathbf{r} - \mathbf{r}') = g \delta(\mathbf{r} - \mathbf{r}') \tag{2}$$

(see also Parkins and Walls, 1998; Leggett, 2001). Here the coupling constant g is given in terms of the s-wave scattering length a in three dimensions and atomic mass m by

$$g = \frac{4\pi\hbar^2 a}{m}. \tag{3}$$

It has been emphasized that g is a parameter depending on particle density (Pieri and Strinati, 2000) as well as on dimensionality (Cherny and Brand, 2004, and references therein). In particular, its dependence on density has been discussed by Pieri and Strinati (2000) in connection with the crossover from wek-coupling BCS

superconductivity to strong-coupling BE condensation (Nozières and Schmitt-Rink, 1985, see also Randeria (1995) for a review).

Returning then to the functional Eq. (1), it is to be noted that for repulsive interactions corresponding to $g > 0$, the functional is convex and the minimum corresponds to the stable ground state. It should be emphasized, for the other case when $g < 0$, that the ground state exists only at weak coupling for a limited number of trapped Bosons, so long as the zero-point energy is able to balance the effect of attractions and prevent collapse.

With this short introduction to the assumed energy functional $E[\Phi]$ set out in Eq. (1), it is then a straightforward matter to perform the minimization with respect to the order parameter $\Phi(\mathbf{r})$. One is then led to the (of course approximate) static GP differential equation having the form of a non-linear Schrödinger equation, namely

$$\left[-\frac{\hbar^2}{2m}\nabla^2 + V_{\mathrm{ext}}(\mathbf{r}) + g|\Phi(\mathbf{r})|^2 \right] \Phi(\mathbf{r}) = \mu\Phi(\mathbf{r}), \tag{4}$$

a condensate at equilibrium being at chemical potential μ.

While we shall consider rather fully below a variety of recent experimental data obtained by some of the present authors, let us briefly summarize at this point just one application of the static GP equation, Eq. (4). The example below follows the work of Castin and Dum (1999) who treated a vortex array. This they obtained by numerical solution of the two-dimensional differential equation for a rotating Bose-Einstein condensate (BEC) under tight vertical confinement. In this rotating condensate, described in the rotating frame by an appropriate static GP equation, one needs to incorporate an inertial term. Then Eq. (4) can be extended to the form

$$\left[-\frac{\hbar^2}{2m}\nabla^2 + V_{\mathrm{ext}}(\mathbf{r}) + g|\Phi(\mathbf{r})|^2 + \Omega L_z \right] \Phi(\mathbf{r}) = \mu\Phi(\mathbf{r}), \tag{5}$$

Ω denoting the rotation frequency and L_z the angular momentum component along the rotation axis. As emphasized in the study of Castin and Dum (1999), the term ΩL_z in Eq. (5) is not diagonal in position or in momentum space, and this implies that numerical solution of Eq. (5) requires special care.

Starting with different trial states, a single-vortex solution, as well as those describing multi-vortex configurations, can be exhibited. In this latter form of solution, the vortices display a tendency to arrange themselves into a triangular geometry, as shown in Fig. 1 which is redrawn from Castin and Dum (1999). As stressed by Minguzzi *et al.* (2004), a significant result which has emerged from solving the static GP Eq. (5) in a cigar-shaped trap is that a vortex line can be bent, as shown in Fig. 17 of Minguzzi *et al.* (2004), following the study of García-Ripoll and Pérez-García (2001). This finding is in general agreement with experimental observations.

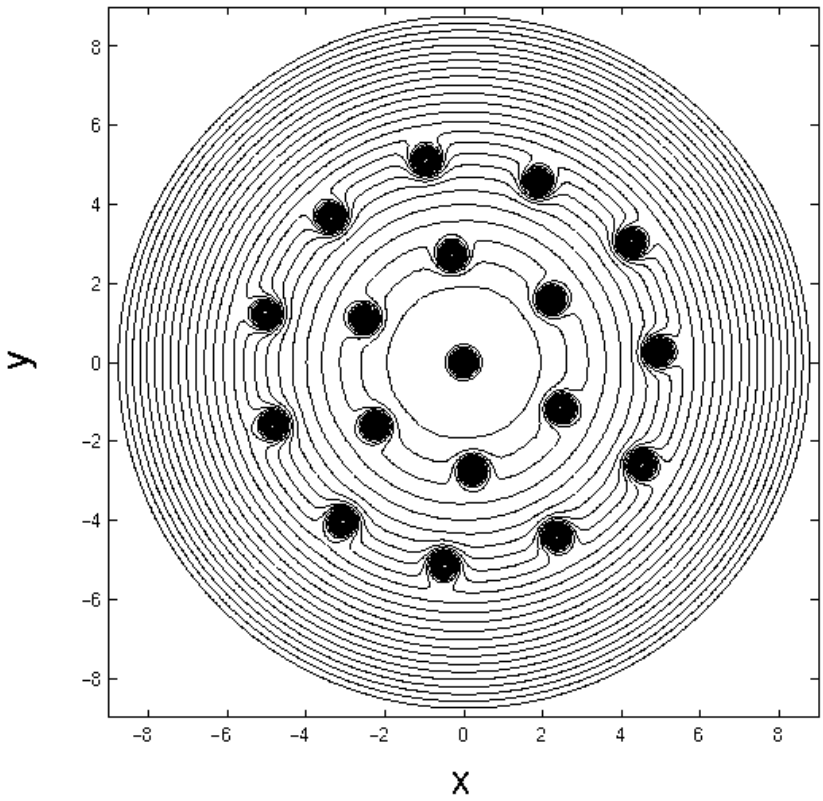

Figure 1: Shows vortex array as exhibited by numerical solution of the static Gross-Pitaevskii Eq. (4) for a rotating Bose-Einstein condensate. Redrawn from Castin and Dum (1999).

2.2 Inhomogeneous Bose superfluids: dynamics using the time-dependent GP equation

Let us proceed to treat in a somewhat parallel manner the dynamics of inhomogeneous trapped superfluid Boson gases. One can make a heuristic generalization of the non-linear Schrödinger equation having the form of the static GP Eq. (4) to describe the now time-dependent condensate wave function $\Phi(\mathbf{r},t)$, to read

$$\left[-\frac{\hbar^2}{2m}\nabla^2 + V_{\rm ext}(\mathbf{r}) + g|\Phi(\mathbf{r},t)|^2\right]\Phi(\mathbf{r},t) = i\hbar\frac{\partial}{\partial t}\Phi(\mathbf{r},t) \tag{6}$$

which, of course, reduces to the static Eq. (4) on making the substitution $\Phi(\mathbf{r},t) = \Phi(\mathbf{r})\exp(-i\mu t/\hbar)$. Eq. (6), also given by Gross (1961, 1963) and Pitaevskii (1961), will be discussed in some detail below, in order to gain further insight into the

realm of validity. Following Dalfovo *et al.* (1999), let us write down the many-body Hamiltonian $\hat{H}$, in second quantization, which describes N interacting Bosons confined again by an external potential $V_{\rm ext}$. This reads:

$$\begin{aligned}\hat{H} &= \int d\mathbf{r}\hat{\Psi}^\dagger(\mathbf{r})\left[-\frac{\hbar^2}{2m}\nabla^2 + V_{\rm ext}(\mathbf{r})\right]\hat{\Psi}(\mathbf{r}) \\ &\quad + \frac{1}{2}\int\int d\mathbf{r}d\mathbf{r}'\hat{\Psi}^\dagger(\mathbf{r})\hat{\Psi}^\dagger(\mathbf{r}')U(\mathbf{r}-\mathbf{r}')\hat{\Psi}(\mathbf{r}')\hat{\Psi}(\mathbf{r}), \qquad (7)\end{aligned}$$

where $U(\mathbf{r}-\mathbf{r}')$ is the two-body interatomic potential already referred to. In Eq. (7), $\hat{\Psi}(\mathbf{r})$ and $\hat{\Psi}^\dagger(\mathbf{r})$ are the Bosonic field operators in the Schrödinger representation ($t = 0$, say). Then, it follows that the evolution equation for the operator $\hat{\Psi}(\mathbf{r}, t)$ takes the form

$$i\hbar\frac{\partial}{\partial t}\hat{\Psi}(\mathbf{r},t) = \left[-\frac{\hbar^2}{2m}\nabla^2 + V_{\rm ext}(\mathbf{r}) + \int d\mathbf{r}'\hat{\Psi}^\dagger(\mathbf{r}',t)U(\mathbf{r}-\mathbf{r}')\hat{\Psi}(\mathbf{r}',t)\right]\hat{\Psi}(\mathbf{r},t). \qquad (8)$$

For a very dilute and fully Bose-Einstein condensed gas at $T = 0$, it is assumed that the field operator can be replaced by the classical field $\Phi(\mathbf{r}, t)$. Taking again the description of $U(\mathbf{r}-\mathbf{r}')$ in Eq. (2) with g related to the s-wave scattering length a by Eq. (3), one is led back to the time-dependent GP Eq. (6).

It is known that the time-dependent GP equation, because it omits dissipation, is not appropriate to deal with the dynamics of a confined Bose gas when quantum depletion or thermal excitations play a significant role. As examples of such situations, one may cite condensate formation and decay, phase coherence, damping of collective motions and excitations from a non–mean-field ground state. Nevertheless, the time-dependent GP Eq. (6) has been found valuable in treating a variety of dynamical processes in condensate clouds. One may cite, as examples, collective-mode frequencies in harmonic or optical-lattice confinement, interference phenomena, dynamics of vortices, propagation of solitons, shock-wave dynamics, four-wave mixing, atom-laser output, as well as expansion of a rotating condensate.

While numerous examples of the use of both GP Eqs. (4) and (6) will be given below in Sec. 3, one immediate illustration to show the usefulness of Eq. (6) will be taken from the work of Chiofalo *et al.* (1999). Their extensive numerical study of drop emission from an optical lattice under gravity was motivated by the experiment of Anderson and Kasevich (1998). In their experiment, an almost pure BEC was poured from a magneto-optic trap into a vertical optical lattice which was produced by a detuned standing wave of light from the counter-propagating laser beams. The gravitational force tilts the lattice potential and drives tunnelling from well states to the continuum. Interference taking place between coherent blobs of condensate at different lattice sites leads to the appearance of falling drops, which can be regarded as coherent matter-wave pulses by analogy with a mode-locked photon laser. Analogous to the laser cavity is the Brillouin zone in momentum space, so that the modulation interval for the pulsed emission of drops equals the period of

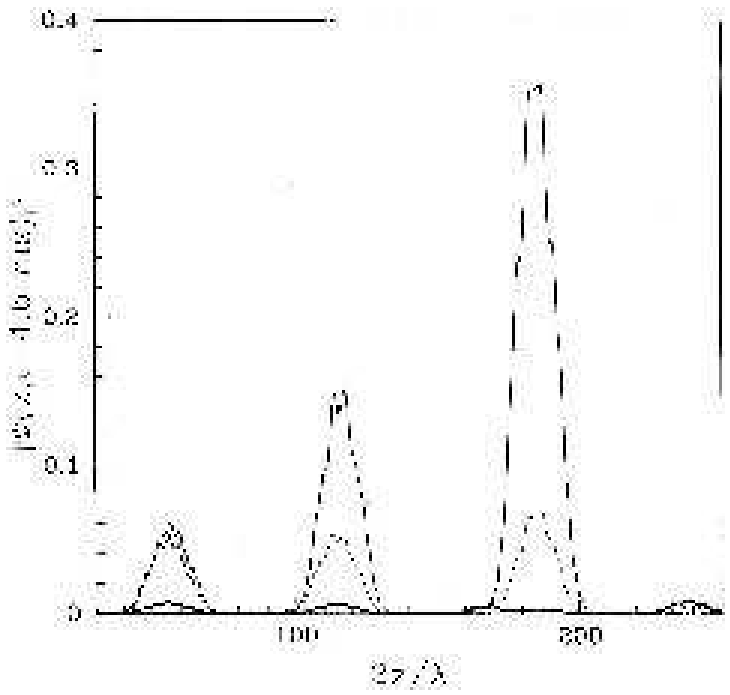

Figure 2: Plots shown relate to condensate drop emission from an optical lattice under gravity. Actually shown is the density profile of the condensate drops after 4.6 ms as a function of a (suitably scaled) distance z in the non-interacting limit. The central condensate around $z = 0$ has been substracted out. Different curves plotted are characterized by increasing well depths, going from shallow (intermediate thickness curve) to deep (thickest curve). Redrawn from Chiofalo *et al.* (1999).

Bloch oscillations. The time interval between successive drops was 1.1 ms in both the experiment and the numerical study, which is the period of Bloch oscillation for a quasi-particle (the whole coherent condensate) driven by the constant force of gravity through a periodic array of potential wells having a lattice period of one-half of the laser wavelength λ.

Primary attention was paid by Chiofalo *et al.* (1999) in their numerical investigations to the part played by atomic interactions in this example of coherent transport. In agreement with band-structure theory of transport in periodic structures, the period of drop emission depends only on the intensity of the drive and the lattice spacing. The size and shape of the emitted drops are instead determined by the magnitude of the lattice barrier and the interatomic forces. In Fig. 2, redrawn from Chiofalo *et al.* (1999), the density profile of the drops emitted from a non-interacting BEC after 4.6 ms is depicted as a function of a suitably scaled distance z. The main condensate around $z = 0$ has been subtracted, the curves being characterized by values of the lattice barrier height. In the experiment, the latter is determined by

the intensity of the optical beams.

When the constant drive is supplemented by a monochromatic oscillating drive, it turns out that the equations governing this form of coherent BEC transport in the linear non-dissipative regime can be mapped onto those for the ac superconducting current flowing across a weak-link Josephson junction (Chiofalo and Tosi, 2001). The voltage drop across the junction is, in essence, replaced by the product of the constant component of the force times the lattice spacing, and the frequency of the Bloch oscillations is in resonance with integer multiples of the oscillating drive frequency. Burger *et al.* (2001) have carried out the relevant experiment on a BEC confined in a magnetic trap plus an optical lattice, the oscillating force being generated by a rapid shift of the centre of the trap.

With this introduction to both static and time-dependent GP differential equations given in Eqs. (4) and (6) respectively, we turn next to discuss a variety of recent experiments by some of the present authors, and the relevance of these GP equations to their interpretation.

3 Selected experiments brought into contact with GP equations

The first experimental realization of a Bose–Einstein condensate (BEC) in a dilute gas of rubidium atoms (see Inguscio *et al.*, 1998, as a general reference) has marked the birth of a completely new field of optics, that of coherent matter wave beams. Indeed, it was immediately recognized that a BEC is in very many aspects the analogue of an optical laser for atoms. After the first pioneering experiment at MIT where a pulsed atom laser was created by simply switching off the confining magnetic potential (Mewes *et al.*, 1997), other more refined experiments followed. The first continuous wave *atom laser* was realized in Munich by coupling atoms out of a magnetic trap using a radio frequency field (Bloch *et al.*, 1999), while in Yale a BEC was loaded into a vertical standing wave to produce the analogue of a mode-locked laser (Anderson and Kasevich, 1998). Coherent matter wave beams were soon shown to produce interference fringes by Andrews *et al.* (1997), and double slit and multiple beam interferometers were soon realized (Fort *et al.*, 2001; Pedri *et al.*, 2001). On the other hand atoms, at variance with photons, interact even in the dilute gas limit. The nonlinearity introduced by atomic interactions in coherent matter waves propagation through vacuum was readily shown to be the same of the third order susceptibility for electromagnetic waves propagating through a nonlinear crystal. It was soon demonstrated that it was indeed possible to observe matter wave amplification (Kozuma *et al.*, 1999; Inouye *et al.*, 1999) and four wave mixing (Deng *et al.*, 1999). More recently, the intrinsic nonlinearity of condensates was successfully exploited in the observation of dark (Burger *et al.*, 1999; Denschlag *et al.*, 2000) and bright solitons (Khaykovich *et al.*, 2002). The last result could also be obtained by controlling the dispersion of matter waves using a

periodic potential (Eiermann *et al.*, 2003).

3.1 Standard experimental procedures

A dilute gas of particles can be cooled to a temperature such that the de Broglie wavelength associated to each particle becomes larger than the mean interparticle distance. At these temperatures the quantum statistics of the particles fully dominates the behaviour of the gas. In a trapped atomic gas of bosons all the particles will tend to occupy the trap state with the largest population in a very similar way to photons in a laser cavity being pulled to the mode with the highest gain. In thermal equilibrium the state with the highest occupancy is the ground state of the trap. In a gas of interacting bosons, however, the ground state of the system will not necessarily be the ground state of the potential holding the atoms. In a dilute ultracold atomic gas of bosons only binary collisions are allowed and the system is conveniently described by the Gross–Pitaevskii equation (4) for the atomic density amplitude. In particular, it is possible to change the value of the s-wave scattering length a by different orders of magnitude and even change its sign by tuning a magnetic field thanks to Fano-Feshbach resonances (Inguscio, 2003). The parameter a strongly influences the properties of the condensate. Condensates with negative a are unstable but can form bright solitons. On the other hand, the ground state of condensates with repulsive interactions ($a > 0$) significantly differs from the ground state of the confining potential. Indeed, for most experimentally realized condensates the nonlinearity totally dominates dispersion, *i.e* the interaction energy is much larger than the kinetic energy. The condensate wavefunction then takes the so called Thomas-Fermi shape which has the same symmetry of the trapping potential and, for a condensate in a harmonic trap, is an inverted parabola (Dalfovo *et al.*, 1999).

The standard experimental procedure for the creation of a Bose-Einstein condensate in a dilute atomic gas starts with laser cooling of an atomic vapor in ultra-high vacuum conditions. This first step, performed in a magneto-optical trap (Raab *et al.*, 1987), takes the atoms from a phase space density of 10^{-20} at room temperature to 10^{-5} below 100 μK. At this phase space, density laser cooling stops essentially because of spontaneous light scattering from the atoms (Chu, 1998; Cohen-Tannoudji, 1998; Phillips, 1998). For this reason, the following cooling step has to be performed in a non-dissipative trap created either by a magnetic field or by a very far-off resonance laser beam. In non-dissipative traps, cooling is achieved by removing the high energy tail of the atomic distribution and by letting the atoms thermalize via binary collisions. Removal of atoms is realized either by reducing the trap depth in optical traps or by RF-induced transitions to untrapped Zeeman sublevels in magnetic traps.

Let us concentrate on magnetic traps. The interaction energy of an atom in a magnetic field is $E = -\boldsymbol{\mu} \cdot \mathbf{B}$, where $\boldsymbol{\mu}$ is the atomic dipole moment. Of the atomic ground sublevels, only low-field seeking states can be trapped in a magnetic

field minimum. If the atomic motion is not very fast, the atomic dipole adiabatically follows the magnetic field. Therefore the energy is proportional to the modulus of the field. However, if the field variation is very rapid, adiabaticity cannot be maintained and atoms are lost from the trap. To avoid these so called *Majorana spin-flips,* it is necessary to avoid a zero of the magnetic field in the trap. Conventional magnetic traps are realized with a few centimeter size coils carrying more than 100 Ampere of current. In this way traps with $10 - 100$ Hz oscillation frequencies are realized.

The cooling procedure, known as *evaporative cooling,* strongly relies on atomic collisions and can be very different for different atomic species. In particular, since the most probable collisions at temperatures below 1 mK are spherically symmetric binary collisions, due to the Pauli principle (DeMarco *et al.*, 1998), this method cannot work for spin-polarized fermions as those trapped in a magnetic trap. Indeed, fermions were cooled to degeneracy either using spin mixtures (DeMarco and Jin, 1999) or via collisions with a bosonic atomic species (Truscott *et al.*, 2001; Schreck *et al.*, 2001; Hadzibabic *et al.*, 2002; Roati *et al.*, 2002).

3.2 Optical dipole potentials

Matter wave beams can be manipulated in very much the same way as optical beams. However, the role of matter and electromagnetic fields is totally reversed in the field of atom-optics. Indeed, condensates can be manipulated with conservative potentials created either by far-off resonance laser beams or by magnetic fields. In the first case the potential is obtained via the interaction of the induced atomic dipole with the electric field of the laser. This dipole potential is dependent on the laser intensity and detuning and for a two level atom in interaction with a far-off resonance beam can be written as

$$V(\mathbf{r}) = \frac{3\pi c^2}{2\omega_0^3}\frac{\Gamma}{\Delta}I(\mathbf{r}), \tag{9}$$

where ω_0 is the atomic resonance frequency, Γ the natural linewidth of the atomic transition, Δ the laser detuning from resonance, and $I(\mathbf{r})$ the intensity of the laser-beam. From Eq. (9) we note that when the laser detuning is negative, atoms are pulled towards the region with the highest laser intensity. On the other hand, when the detuning is positive, atoms are expelled from high intensity regions. This can be used to create very different kind of potentials with a single tunable laser beam. For example, it is possible to create atomic waveguides either by using collimated gaussian laser beams with negative detuning, or collimated hollow laser beams with positive detuning (Bongs *et al.*, 2001b).

With a sheet of light created by rapidly moving a collimated laser beam with an acousto-optic modulator, the group of IQO–Hannover has been able, by simply varying the laser beam intensity, to create an atom mirror, a beam-splitter, or a phase-shifter (see Fig. 3). The laser detuning for these experiments was positive.

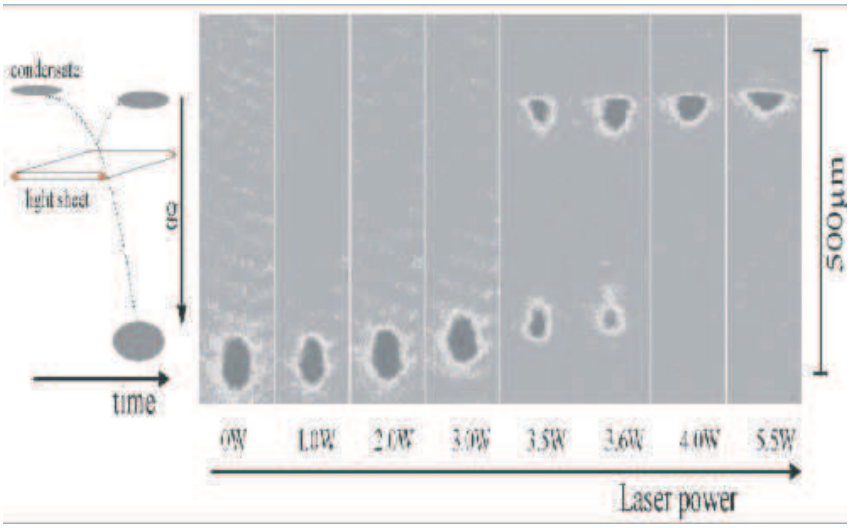

Figure 3: Scheme of the IQO experiment. The condensate falls under the effect of gravity and bounces off the potential generated by the laser light.

The experiment was performed by creating a condensate via evaporative cooling in a magnetic trap (Inguscio *et al.*, 1998) and then dropping it under the effect of gravity onto the sheet of light. When the laser intensity was very high, the atoms did not acquire sufficient kinetic energy during their fall to go over the dipole potential and were totally reflected (Bongs *et al.*, 1999). When the laser intensity was reduced, part of the atoms could go over the dipole potential and the system realized a beam-splitter. By further reducing the laser intensity all the atoms were able to go over the potential but were retarded with respect to free fall in analogy to an optical phase-shifter (Bongs *et al.*, 2001a).

3.3 Atom chips and magnetic microtraps

These examples demonstrate that laser radiation is a very versatile tool, since it is possible to create many different potentials simply from the interference of laser beams coming from different directions as will be discussed below. On the other hand, it is also possible to manipulate atoms with magnetic field gradients. Magnetic traps are, for neutral atoms, a particularly versatile class of these manipulation methods as they can be used for any atomic species with a magnetic moment and they can produce conservative potentials also for very long times. Techniques to trap and manipulate atoms with magnetic fields once integrated with surface deposition techniques, either lithographic or of other kind, realize what is termed an *atom chip* (Folman *et al.*, 2000). *Atom chips* are based on the possibility of creating a 2D-quadrupole magnetic field close to a current carrying wire by compensating the field generated by the wire $B = \frac{\mu_0}{\pi}\frac{I}{r}$ at the height z_0 with a constant magnetic field. If

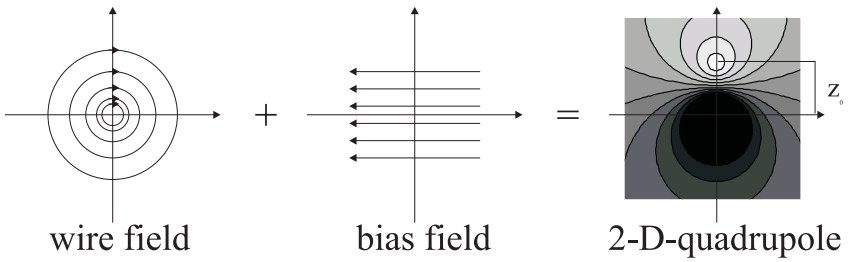

Figure 4: Using a bias field to compensate at a point z_0 the magnetic field generated by a current carrying wire, it is possible to create a 2D-quadrupole trap.

the magnetic moment $\boldsymbol{\mu}$ of the atom remains aligned with the magnetic field the resulting potential for the atoms can be approximated as

$$V = \mu \frac{\mu_0 I}{\pi z_0^2}(|z_0 - z| + |y|), \tag{10}$$

where we have assumed the wire to be along the x axis. With a current of just 0.4 A in the wire and a constant field of 35 G, it is possible to create a waveguide with a confining frequency of 10 kHz for ^{87}Rb much larger than conventional magnetic traps.

The wire guide represents the building brick for magnetic microtraps. Indeed, by bending the wire in a U shape as illustrated in Fig. 5 (b), it is possible to create a 3D quadrupole. As already pointed out, this trap configuration have high atomic losses due to Majorana spin-flips. In order to avoid these losses, it is better to create a harmonic trap with a filed minimum different from zero as can be done by bending the wire in a Z shape [Fig. 5 (a)]. The bias field can also be realized in a planar configuration using three parallel wires with opposite currents as in Fig. 5 (d). This configuration can then be used to create more complicated structures as in Fig. 5 (c), where a possible analogue of a SQUID is illustrated.

These devices represent one of the most promising schemes for coherent atom optics and may be the basis for a totally new class of integrated sensors and quantum logic instruments. Indeed, thanks to component miniaturization, in *atom chips* it is possible to reach huge field gradients (above 1 Tesla/cm) with 1 Ampere currents, of the same order of magnitude as those used in electronic circuits and a few orders of magnitude lower than those employed in conventional apparatuses. Furthermore, the substrates employed are compatible with the ultra-high vacuum technology needed for atom cooling. Nowadays the microstructures used experimentally are rather simple and the conductors sizes are of the order of 10 μm with a total chip size of a few cm^2. However, they are capable of substituting experimental systems currently spread in about 1 m^3. Integrating many elements to control atoms onto a single device, an *atom chip*, will make atom physics experiments much more robust and simple. This may allow much more complicated tasks in atom manipulation to

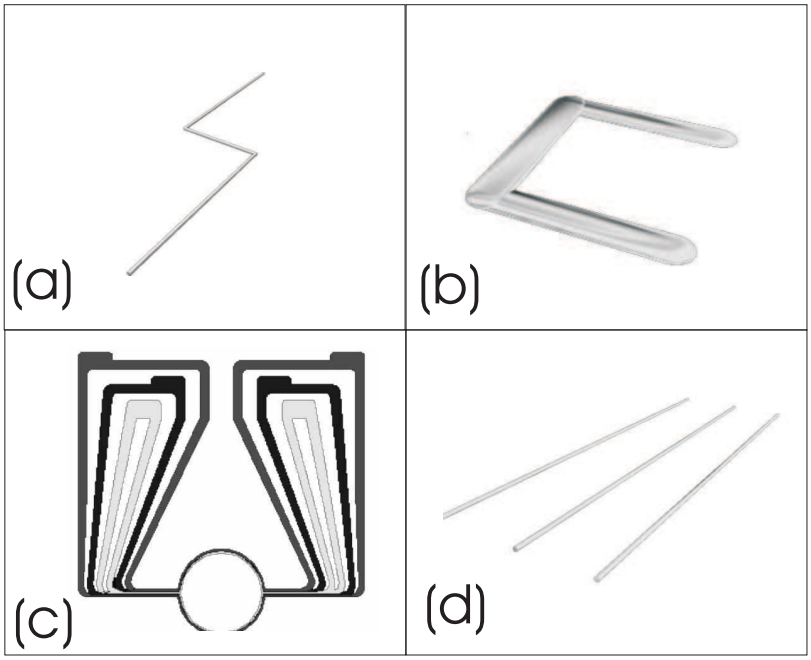

Figure 5: Various microtrap configurations: (a) Z-Trap; (b) U-Trap. Both the Z-Trap and U-Trap need an external bias field to achieve a 3D-confining potential for cold atoms; (c) A ring guide with two diametral potential barriers, working with cold atoms like a SQUID works with superconductors; (d) A linear guide completely realized in planar geometry, without any bias field.

be performed in a way similar to how integration of electronic elements has allowed the development of new powerful electronic devices. Ideally, one desires routine single atom state selective loading, preparation and manipulation. All will be achieved with minimal heat load and power consumption. Potentials with sizes smaller than the particle de Broglie wave-length will allow tight traps with large energy level spacing. The large level spacing reduces the probability of the environmental noise to induce unwanted excitations. Consequently, coherent manipulation will be more stable. Using well developed nanofabrication technology from microelectronics to build the atom optics will allow integration of many atom optical devices into complex quantum networks combining the best of two worlds: the ability to use cold atoms, a well controllable quantum system, and the immense technological capabilities of nanofabrication and microelectronics to manipulate the atoms. Experiments based on *atom chips* have allowed the demonstration of trapped atom interferometers (Hänsel *et al.*, 2001c), of *atomic conveyor belts* (Hänsel *et al.*, 2001b), and of atomic waveguides (Folman *et al.*, 2000). Currently one of the main concerns in *atom chips* is the possibility of maintaining a coherent sample close to a surface. After the achievement of BEC with these devices (Hänsel *et al.*, 2001a; Ott *et al.*,

2001), it was discovered a fragmentation of the atomic cloud when brought close to the surface (Fortágh *et al.*, 2002). This fragmentation was very recently attributed to the thickness fluctuations of the conductors (Esteve *et al.*, 2004), which causes the current to deviate from a straight line producing unwanted axial magnetic fields. Other experiments are concentrating on surface induced losses (Jones *et al.*, 2003; Harber *et al.*, 2003; Lin *et al.*, 2004), however it was possible to realize an atomic clock starting from a BEC in an atom chip (Treutlein *et al.*, 2004).

3.4 BEC in periodic potentials

We now describe some experiments performed on BECs in periodic potentials, that well demonstrate the flexibility of optical potentials in the manipulation of condensates. In their experiment, Fort *et al.* (2000) load cold ^{87}Rb atoms in the $|F = 1\, m_F = -1\rangle$ state from a double magneto-optical trap system into a Ioffe type harmonic magnetic trap. The trap is cylindrically symmetric with an axial frequency of $\omega_x/2\pi = 9$ Hz and a radial frequency of $\omega_\perp/2\pi = 92$ Hz. Fort *et al.* (2000) then cool the atoms in this trap via rf-forced evaporation until they reach a temperature below 300 nK, just above the critical temperature for condensation, which is around 150 nK dependent on the number of atoms we load in the trap. At this stage of evaporation they suddenly switch on an optical standing wave formed by retroreflecting light from a laser blue detuned of ~ 3 nm with respect to the D_1 transition at $\lambda = 795$ nm. The laser beam is aligned horizontally along the axis of the magnetic trap and, since the laser beam waist is much larger than the atomic cloud transverse size and does not produce any appreciable radial force, forms an array of disk shaped traps together with the magnetic potential.

The potential is therefore

$$V = \frac{1}{2}m(\omega_x^2 x^2 + \omega_\perp^2 r_\perp^2) + sE_R \cos^2(2\pi x/\lambda). \tag{11}$$

The optical potential is given in units s of the energy $E_R = h^2/2m\lambda^2$ gained by an atom (of mass m) absorbing one lattice photon corresponding in rubidium to a temperature of ~ 170 nK. In these experiments the optical potential could be varied up to $s = 15$. When $s \gg 1$ the atoms are confined in an array of classically independent traps since the optical potential barriers are much higher than the thermal energy of the atoms. Indeed it is possible to "freeze" the degree of freedom associated with the motion along the axis and study condensation in this quasi 2D system (Burger *et al.*, 2002). After switching on the laser light we continue the evaporation ramp until the desired temperature is reached. This ensures that the atoms reach the equilibrium state in the combined trap. When we evaporate to well below the critical temperature, so that no thermal fraction is experimentally visible, we typically obtain ~ 200 condensates separated by a distance of $\lambda/2$, each containing ~ 1000 atoms. Due to the blue detuning of the laser beam the atoms are trapped in the nodes of the standing wave reducing light scattering below ~ 1 Hz.

When the height of the optical barriers is much larger than the condensates chemical potential we are justified in describing the condensate as a sum of wave-functions localized in each potential well:

$$\Psi_0(\mathbf{r}) = \sum_{k=0,\pm 1 \ldots \pm k_M} \exp[-(x - k\lambda/2)^2/2\sigma^2 + i\phi_k] \frac{\sqrt{2}}{g} \mu_k \left(1 - \frac{r_\perp^2}{(R_\perp)_k^2}\right), \qquad (12)$$

where $(R_\perp)_k = \sqrt{2\mu_k/m\omega_\perp^2}$ is the radial size of the k-th condensate, g depends on the scattering length a through Eq. (3), while $\mu_k = \frac{1}{2} m\omega_x^2 d^2 \left(k_M^2 - k^2\right)$ plays the role of an effective k-dependent chemical potential. The value of k_M is fixed by the normalization condition $N = \sum N_k$ to

$$k_M^2 = \frac{2\hbar\overline{\omega}}{m\omega_x^2 d^2} \left(\frac{15}{8\sqrt{\pi}} N \frac{a}{a_{ho}} \frac{d}{\sigma}\right)^{\frac{2}{5}},$$

with $\overline{\omega} = (\omega_x \omega_\perp^2)^{1/3}$ the geometrical average of the magnetic frequencies, $a_{ho} = \sqrt{\hbar/m\overline{\omega}}$ is the corresponding oscillator length. From the above equations one also obtains the result $N_k = N_0(1 - k^2/k_M^2)^2$ with $N_0 = \frac{15}{16} N/k_M$. Equation (12) generalizes the well known Thomas-Fermi results holding for magnetically trapped condensates (Dalfovo *et al.*, 1999) to include the effects of the optical lattice. This generalization is justified by the fact that the optical confinement along the optical lattice is much stronger than the magnetic potential therefore it is more suitable to use a harmonic approximation for the wave-function along the x-direction and a Thomas-Fermi approximation in the radial direction (Pedri *et al.*, 2001).

When the atoms are released from the combined trap they spread out and overlap producing an interferogram which will depend on the relative phases ϕ_k of the individual condensates. In Fig. 6 (A), we show a typical image of the cloud taken after an expansion time $t_{\rm exp} = 29.5$ ms, corresponding to a total number of atoms $N \simeq 20000$ and to an optical potential $s = 5$. The image shows a clear structure with three interference peaks separated by $2h/m\lambda t_{\rm exp}$, *i.e.* by the distance corresponding to the reciprocal of the lattice constant. We remark that, differently from the case of two separated condensates, interference fringes appear only if the initial configuration is mutually coherent. In other words, since one single interference experiment with an array of condensates is equivalent to averaging a series of interference experiments with two condensates, an interference pattern will appear only in presence of a fixed relative phase between condensates belonging to consecutive wells. What is locking the phase difference across the array of BEC is tunnelling through the optical barriers, in a classical picture no interference peaks would arise. The width of the central peak ($n = 0$) of the interferogram is of the order $\Delta p_x \sim \hbar/mR_x t_{\rm exp}$ where $R_x \sim k_M d$ is half of the length of the whole sample in the x-direction. The occurrence of these peaks is the analogue of multiple order interference fringes in light diffraction.

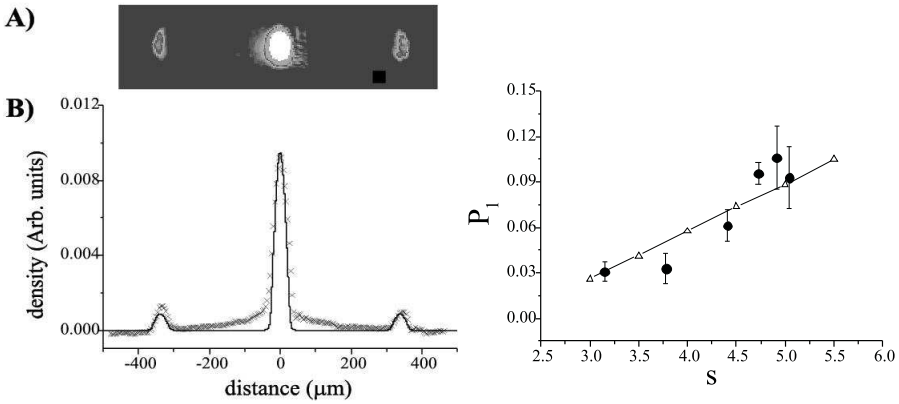

Figure 6: *Left:* (A) Absorption image of the density distribution of the expanded array of condensates. (B) Experimental density profile (crosses) obtained from the absorption image (A) integrated along the vertical direction. The wings of the central peak result from a small thermal component. The continuous line corresponds to the calculated density profile for the expanded array of condensates for the experimental parameters ($s = 5$ and $t_{\rm exp} = 29.5$ ms). *Right:* Experimental (circles) and theoretical (triangles) values of the relative population of the $n = 1$ peak with respect to the $n = 0$ central one as a function of the intensity factor s of the optical potential $V_{\rm opt}$.

The relative population of the $n \neq 0$ peaks with respect to the central one ($n = 0$) obeys the simple law

$$P_n = \exp(-16\pi^2 n^2 \sigma^2/\lambda^2), \tag{13}$$

holding also in the presence of a smooth modulation of the atomic occupation number N_k in each well. Equation (13) shows that, if σ is much smaller than $\lambda/2$, the intensity of the lateral peaks will be high, with a consequent important layered structure in the density distribution of the expanding cloud. The value of σ, which characterizes the width of the condensates in each well, is determined, in first approximation, by the optical confinement. By using a numerical minimization of the energy we can determine the relative population P_n of the $n = 1$ peak as a function of the intensity factor s. This is shown in Fig. 6 (right) together with the experimental results. The good comparison between experiment and theory reveals that the main features of the observed interference patterns are well described by this model.

3.5 Josephson Junction array with BECs

In the preceding subsection we have shown that the BECs produced in the combined trap are phase-locked by the tunnelling of atoms through the optical barriers. The system indeed realizes a one-dimensional array of Josephson Junctions (JJs), as we wish to demonstrate in this section (Cataliotti *et al.*, 2001).

A Josephson junction is a simple device made of two coupled macroscopic quantum fluids (Barone and Paterno, 1982; Barone, 2000). If the coupling is weak enough, an atomic mass current I flows across the two systems, driven by their relative phase $\Delta\phi$ with a limiting current I_c, the "Josephson critical current", namely the maximal current allowed to flow through the junction. The relative phase dynamics, on the other hand, is sensitive to the external and internal forces driving the system being driven by the chemical potential difference between the two quantum fluids (Tilley and Tilley, 1990). The arrays of JJs are made of several simple junctions connected in various geometrical configurations. In the last decade, such systems have attracted much interest, due to their potential for studying quantum phase transitions in systems where the external parameters can be readily tuned (Fazio and van der Zant, 2001). Recently, the creation of simple quantum-logic units and more complex quantum computer schemes have also been discussed (Makhlin *et al.*, 2001).

The condensates in two neighbouring sites of the array have a significant interaction via the tunnelling through the barrier, we can therefore rewrite the time-dependent Gross-Pitaevskii equation (6), normally used to describe weakly interacting condensates, as a discrete non-linear Schrödinger (DNLS) equation in a parabolic potential (Trombettoni and Smerzi, 2001). We remark that the model used here is one dimensional, as we are now only concerned with the motion along the array. We write the condensate order parameter as $\Psi(x,t) = \sum_j \sqrt{N_j(t)}\, e^{i\phi_j(t)} \Phi_j(x)$ and obtain

$$i\hbar \frac{\partial \psi_n}{\partial t} = -K(\psi_{n-1} + \psi_{n+1}) + (\epsilon_n + \Lambda \mid \psi_n \mid^2)\psi_n, \tag{14}$$

where $\epsilon_n = \Omega n^2$, $\Omega = \frac{1}{2} m\omega_x^2 \left(\frac{\lambda}{2}\right)^2$, $\Lambda = g_0 N_T \int dx\, \Phi_j^4$. The tunnelling rate is $K \simeq -\int dx \left[\frac{\hbar^2}{2m} \nabla\Phi_j \cdot \nabla\Phi_{j+1} + \Phi_j V \Phi_{j+1}\right]$. We observe that the wavefunctions Φ_j, as well as the tunnelling rate K, depend on the height of the energy barrier.

In the ground state configuration the Bose-Einstein condensates are distributed among the sites at the bottom of the parabolic trap. If we suddenly displace the magnetic trap along the lattice axis by a small distance ~ 30 μm (the dimension of the array is ~ 100 μm), the cloud will be out of equilibrium and will start to move. As the potential energy that we give to the cloud is still smaller than the inter-well barrier, each condensate can move along the lattice only by tunnelling through the barriers. A collective motion can only be established at the price of a well definite phase coherence among the condensates. In other words, the relative phases among all adjacent sites should remain locked together in order to preserve the ordering of

the collective motion. The locking of the relative phases will again show up in the expanded cloud interferogram.

For not too large displacements, we observe a coherent collective oscillation of the condensates, *i.e.* we see the three peaks of the interferogram of the expanded condensates oscillating in phase thus showing that the quantum mechanical phase is maintained over the entire condensate (Fig. 7, left). In the top part of Figure 7 we show the positions of the three peaks as a function of time spent in the combined trap after the displacement of the magnetic trap, compared with the motion of the condensate in the same displaced magnetic trap but in absence of the optical standing-wave. (We refer to this as to "harmonic" oscillation.) The motion performed by the center of mass of the condensate is an undamped oscillation at a substantially lower frequency than in the "harmonic" case. We remark that in a thermal cloud, although individual atoms are allowed to tunnel through the barriers, no macroscopic phase is present and no motion of the center of mass should be observed. The center of mass positions of the thermal clouds are also reported in Fig. 7 (left) together with the "harmonic" oscillation of the same cloud in absence of the optical potential. As can be clearly seen, the thermal cloud does not move from its original position in presence of the optical lattice.

The current flowing through the junction between two quantum fluids has a maximum value, the critical Josephson current I_c, which is directly proportional to the tunneling rate K. The existence of such a condition essentially limits the maximum velocity at which the condensate can flow through the inter-well barriers and therefore reduces the frequency of the oscillations. As a consequence, we expect a dependence of the oscillation frequency on the optical potential through the tunneling rate. If we rewrite the DNLS equation (14) in terms of the canonically conjugated variables population/phase and use collective coordinates, we arrive to a phase-current relation

$$\hbar \frac{d}{dt} \xi(t) = 2K \sin \Delta\phi(t) \tag{15a}$$

$$\hbar \frac{d}{dt} \Delta\phi(t) = -m\omega_x^2 \left(\frac{\lambda}{2}\right)^2 \xi(t), \tag{15b}$$

where $\xi(t)$ is the center of mass of the array and $\Delta\phi(t)$ the relative phase across the junction. We remark that, in the regimes we are considering, the current-phase dynamics does not depend explicitly on the interatomic interaction. However, it is clear that the non-linear interaction is crucial on determining the superfluid nature of the coupled condensates, by locking the overall phase coherence against perturbations.

From Eqs. 15 we can see that the small amplitude oscillation frequency ω of the current $I \equiv N_T \frac{d}{dt}\xi$ gives a direct measurement of the critical Josephson current $I_c \equiv 2KN_T/\hbar$ and, therefore, of the atomic tunneling rate of each condensate through the barriers. The critical current is related to the frequency ω of the atomic oscillations

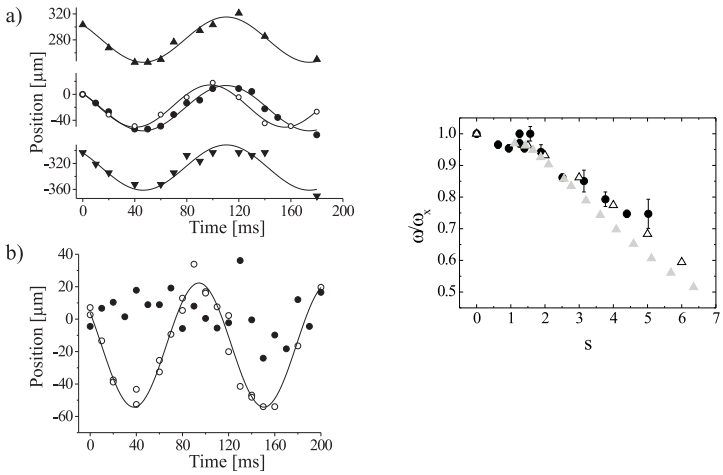

Figure 7: *Left:* (A) Center of mass positions of the three peaks in the interferogram of the expanded condensate as a function of the time spent in the combined trap after displacement of the magnetic field. Up and down triangles correspond to the first order peaks, filled circles to the central peak. Open circles show the center of mass position of the BEC in absence of the optical lattice. The continuous lines are the fits to the data. (B) Center of mass positions of the thermal cloud as a function of time spent in the displaced magnetic trap with the standing wave turned on (filled circles) and off (open circles). *Right:* The ratio of the frequency of the atomic current in the array of Josephson junctions to the harmonic trap frequency as a function of the inter-well potential height. Experimental data (circles) are compared to the values calculated with Eq. (16) (grey triangles) and to a numerical simulation of the 1D GPE (open triangles).

in the lattice and to the frequency ω_x of the condensate oscillations in absence of the periodic field by the relation

$$I_c = \frac{4\hbar N_T}{m\lambda^2}\left(\frac{\omega}{\omega_x}\right)^2 . \tag{16}$$

Figure 7 (right) shows the experimental values of the oscillation frequencies together with the result of a variational calculation. It must be noted that, due to mean field interactions, in our system only for potentials higher than $\sim E_R$ a bound state exists in the lattice.

3.6 Expansion inside a moving 1D optical lattice

We now discuss a different experiment where we study the expansion of a condensate inside a moving 1D optical lattice (Fallani *et al.*, 2003). This experiment allows us to load the condensate with different quasi-momenta q in the periodic structure realized by the optical lattice. We will show how it is possible to adopt a

completely different language, namely that of band structures in solids, to describe the condensate motion. This is possible because the momentum spread in the condensate is so small that the behavior of the entire atomic cloud can be explained as that of a single particle. From solid state physics it is well known that in the presence of an infinite periodic potential the energy spectrum of the free particle is modified and a band structure arises (see *e.g.* Jones and March, 1986). In the rest frame of the lattice the eigenenergies of the system are $E_n(q)$, where q is the quasi-momentum and n the band index. According to band theory, the velocity in the n-th band is $v_n = \hbar^{-1}\partial E_n/\partial q$ and the effective mass is $m^* = \hbar^2(\partial^2 E_n/\partial q^2)^{-1}$. The effective mass can be negative for a range of quasi-momentum and this has been recently recognized as a possibility of realizing bright solitons in BEC with repulsive interactions (Lenz *et al.*, 1994; Konotop and Salerno, 2002; Hilligsø *et al.*, 2002; Eiermann *et al.*, 2003).

In this experiment we first produce the condensate in a pure harmonic trap, then we switch off the magnetic harmonic potential let the BEC expand for 1 ms and we switch on a moving periodic potential. After 1 ms of expansion the density of the condensate decreases enough to neglect the non linear term in the Gross-Pitaevskii equation describing an interacting BEC. This means that, as a first approximation, we are allowed to consider the BEC as a linear probe of the periodic potential energy spectrum. The moving periodic potential is created by the interference of two counterpropagating laser beams with a slightly different frequency and blue detuned 0.5 nm from the D_2 resonance at 780 nm. The two beams are obtained by the same laser and are controlled by two independent acousto-optic modulators. The resulting light field is a standing wave moving in the laboratory frame with a velocity $v_L = \lambda\Delta\nu/2$, where $\Delta\nu$ is the frequency difference between the two laser beams. In our experiment, we typically vary the optical lattice velocity between 0 and $2v_R$ where $v_R = \hbar k_L/m$ is the recoil velocity of an atom absorbing one lattice photon and corresponds, in the frame of the band theory, to the limit of the Brillouin zone. We switch on the moving optical lattice adiabatically by ramping the intensity of the two laser beams in 2 ms. This ensures we are loading the condensate in a Bloch state of well-defined energy and quasi momentum (Denschlag *et al.*, 2002). We let the condensate expand in the lattice and after a total expansion time of 13 ms we take an absorption image of the cloud along the radial horizontal direction looking at the position and dimensions of the condensate inside the optical lattice. From the position after the expansion, we extract the velocity of the condensate inside the optical lattice. In particular, we repeat the experiment for different velocities of the lattice and compare the position of the expanded condensate inside the lattice with the position of the condensate expanded without the optical lattice. Let us call Δz the difference in position along the axial direction. Then, the velocity of the BEC inside the optical lattice is given by $v = \Delta z/\Delta t - v_L$, where Δt is the expansion time inside the lattice.

In Fig. 8 we show the results obtained for the velocity of the condensate as a

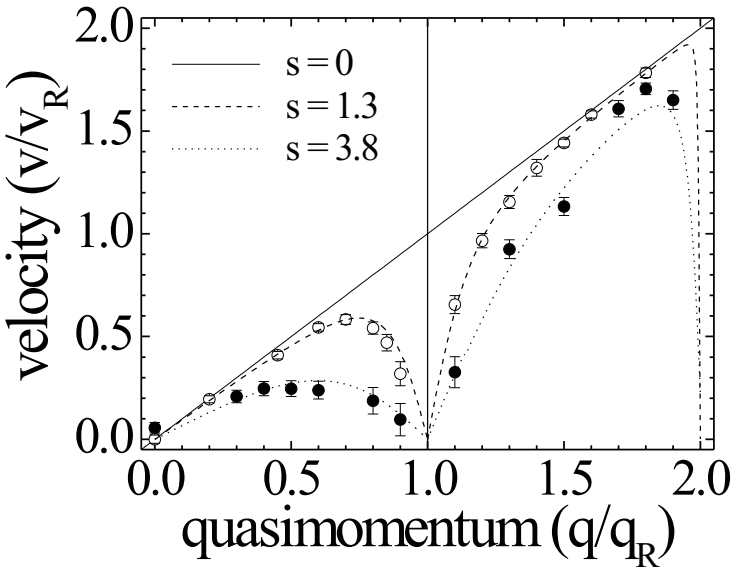

Figure 8: Velocity of the condensate inside the optical lattice as a function of the quasi-momentum q in units of the recoil momentum $q_R = \hbar k_L$. The open circles corresponds to data obtained with $V_{\rm opt} = 1.3E_R$ and the filled circles to data obtained with $V_{\rm opt} = 3.8E_R$. The dashed and dotted lines are the correspondent curves given by the band theory.

function of the quasi-momentum q for two different values of the lattice potential depth. The experimental data points are compared with the theoretical results obtained from the band theory and show a very good agreement. With an adequate sampling of the velocity we can extract the effective mass values given by $\partial v/\partial q$. The results for an optical potential depth of 1.3 E_R are shown in Fig. 9. As we increase the lattice velocity (corresponding to increasing the quasi-momentum q) the effective mass rapidly increases and between 0.7 q and 0.8 q it first becomes infinite positive and then negative.

The consequence of the strong variation of the effective mass is expected to consistently modify the expansion of the condensate along the axial direction (Massignan and Modugno, 2003). As a matter of fact, the effective mass enters the diffusive (kinetic) term in the Gross-Pitaevskii equation.

In Fig. 10 we report the radii of the condensate measured as a function of the quasi-momentum after the expansion inside the optical lattice compared to numerical predictions based on an effective 1D theoretical model (Massignan and Modugno, 2003). The axial radius (filled circles in Fig. 10) decreases until the quasi-momentum

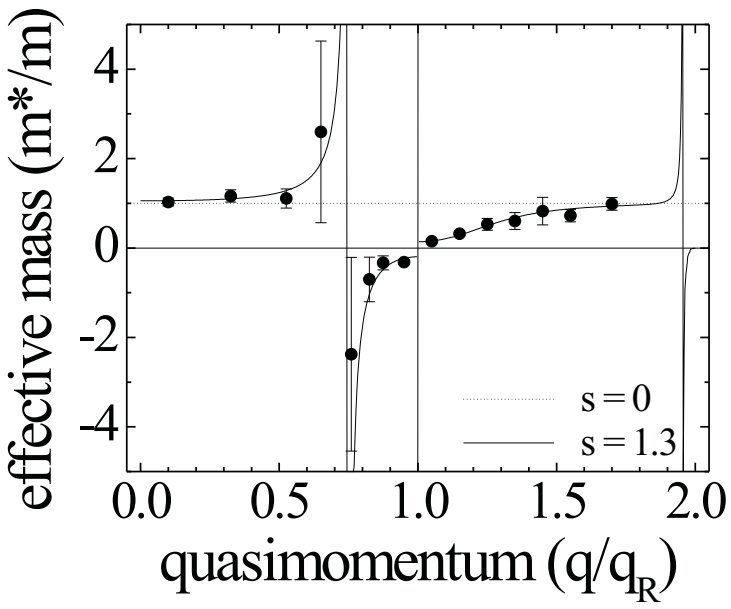

Figure 9: Effective mass of a condensate moving in an optical lattice of $1.3E_R$ as a function of the quasi-momentum. The data points correspond to the values extracted from the measured velocity and the solid line is the corresponding theoretical prediction of the band theory.

reaches q_R. This is first due to the increase of the effective mass (causing a slower expansion) and then by the fact the the effective mass becomes negative (causing a contraction of the axial direction during the time spent in the optical lattice).

When $q > q_R$, the effective mass becomes positive again but with a value smaller then the real mass m. As a consequence the expansion becomes faster in this region of quasi-momenta. In Fig. 10 we also report the measured values of the radial dimension of the BEC. A deviation from the expansion without optical lattice (dashed line) is observed also in this direction for $q < q_R$, even if this dimension is not directly affected by the presence of the lattice. This is consistent with the theory (continuous line) and can by explained in terms of a coupling between the axial and the radial dynamics.

For $q < q_R$, the compression along the lattice direction increases the mean-field energy and causes a faster radial expansion. Instead, when the condensate is loaded with $q > q_R$, the axial expansion is enhanced ($0 < m^* < m$) and the residual mean-field energy is further reduced, causing a suppression of the non-linear coupling between the axial and radial dynamics. This behaviour is evident in the

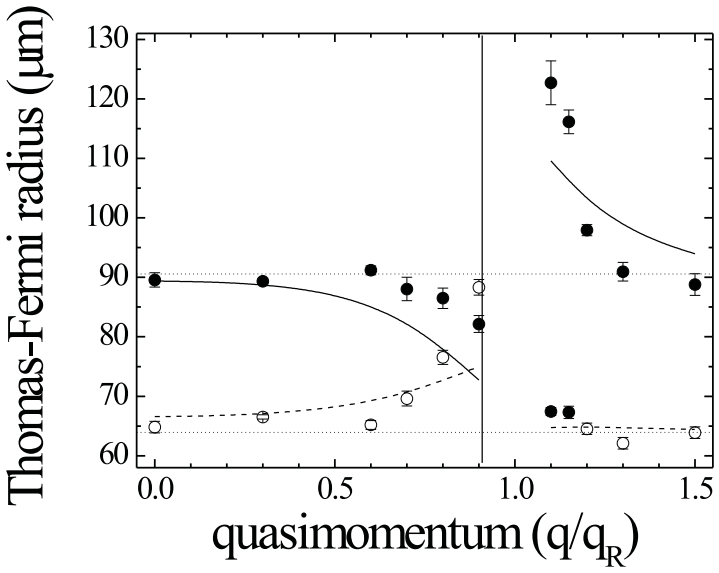

Figure 10: Axial and radial dimensions of the condensate after the expansion in an optical lattice $V_{\rm opt} = 2.9E_R$. The experimental points (filled and open circles) show the Thomas–Fermi radii of the cloud extracted from a 2D fit of the density distribution. The dotted lines show the dimensions of the expanded condensate in the absence of the optical lattice. The continuous and dashed lines are theoretical calculations obtained from the 1D effective model.

absorption images reported in Fig. 11, where we show the shape of the condensate expanded without optical lattice (image **a)**), and with an optical lattice of 2.9 E_R and respectively quasi-momenta $q < q_R$ (**b**)) and $q > q_R$ (**c**)). In the first case, a contraction along the axial direction is accompanied by a faster expansion along the radial direction, while in the second case the condensate expands faster in the axial direction.

3.7 Experiments beyond the GP equation

More recently experiments are starting to explore the possibility of creating and manipulating pure quantum states of many atoms. In a beautiful work, Greiner *et al.* (2002a) have has loaded a BEC in a three-dimensional optical lattice. By adiabatically increasing the periodic potential, it was possible to enter in a regime where the tunnelling between adjacent wells was comparable with the atomic interaction. In this situation, quantum fluctuations of the atom number in each well become relevant and the system can no longer be described by the GP equation. The sys-

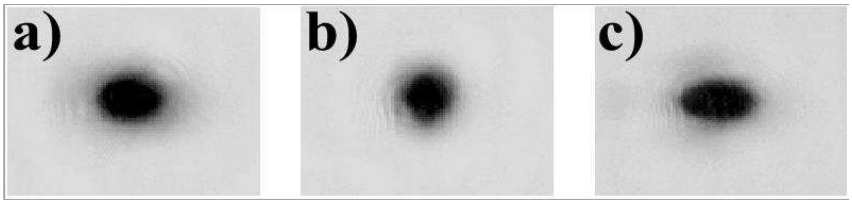

Figure 11: Absorption images of the expanded condensate. From left to right: (a) normal expansion of the condensate without lattice; (b) axial compression in a lattice of 2.9 E_R and $v_L = 0.9 v_R$; (c) enhanced axial expansion in a lattice of 2.9 E_R and $v_L = 1.1 v_R$.

tem undergoes a Mott-insulator quantum phase transition to a state where the atom number in each well is fixed (Jaksch *et al.*, 1998; Sachdev, 1999). In such a situation no interferogram can be recorded when the atoms are released from the potential. In addition, it is not possible to move the atoms through the array any longer until the potential energy difference between two adjacent wells equals the energy necessary to add an atom to an already occupied site.

This experiment, aside from showing the first clear quantum phase transition, opened the path for a new set of experiments where it was possible to show collapses and revivals of the matter wave field, as non-trivial quantum states were formed in the lattice (Greiner *et al.*, 2002b). Later, in the same system, it was possible to create massive entanglement between distant atoms in the lattice by the coherent manipulation of collisions (Mandel *et al.*, 2003) and, more recently, a Tonks-Girardeau gas was observed for the first time (Paredes *et al.*, 2004).

4 Limitations of the GP equations from first-principles arguments

The purpose of this short section is to expose some limitations of the GP equations by appealing to first-principles theory. The most fundamental approach seems to us to be that due to Leggett (2003). The arguments outlined below therefore largely follow his article, though because of space limitations our discussion will be more qualitative than his original study.

His starting point is what he terms the formulation of a 'pseudo-paradox' in the theory of a dilute Bose gas with repulsive interactions. His 'paradox' can be stated as follows. The usual ground-state energy in the GP approximation set out in Section 2 above is lower than that in the Bogoliubov theory.[1] Thus, by standard variational arguments, the GP answer should be an improved approximation to

[1] Concerning the calculation of the ground-state energy of a homogeneous Bose-Einstein condensate beyond Bogoliubov theory, we refer the reader to the works of Lieb and Yngvason (1998); Weiss and Eckardt (2004), and references given therein.

the Bogoliubov result, which contradicts the 'established wisdom' concerning this problem. Leggett (2003) then resolves the 'paradox' by a correct transcription of the two-body scattering treatment to the many-body problem. He stresses that this resolution has not to do with spurious ultraviolet divergences resulting from the replacement of the true interatomic potential by a model δ-function pseudopotential. Instead, Leggett points out that it comes from an infrared divergence which has as a consequence, first of all, that the GP approximation actually has no well-defined many-body wave function underpinning it. Leggett goes on then to show that the 'best' attempt to construct an approximate variational wave function always results in a ground-state energy which either exceeds, or at the very best is equal to, that given by the Bogoliubov approximation.

This all prompts us to follow this brief section with an account of a proposal by Angilella *et al.* (2004) to replace the static GP differential Eq. (4) by an integral equation (Sec. 6). The starting point of their derivation is the Bogoliubov-de Gennes theory, and therefore some physical background to their theory will first be given in Section 5 immediately below.

5 Bogoliubov-de Gennes equations: physical background

A key ingredient of the GP equation is a spatially varying order parameter $\Phi(\mathbf{r})$, describing the inherently inhomogeneous density profile of a BEC condensate. Such an assumption is usually not necessary for a pure, conventional (*i.e., s*-wave) superconductor, for which BCS theory applies with a constant order parameter Δ (see, *e.g.,* Schrieffer, 1964). This is not the case for inhomogeneous superconductors, such as alloys or metals in the presence of impurities, both diluted and isolated, where a position dependent order parameter $\Delta(\mathbf{r})$ is required. Such a generalization is also relevant to describe boundary effects in superconductors, or the effect of a non-uniform magnetic field, as is given by a position dependent vector potential $\mathbf{A}(\mathbf{r})$. The set of coupled equations which relate the inhomogeneous pairing potential $\Delta(\mathbf{r})$ and the self-consistent potential $U(\mathbf{r})$ experienced by single particles in the superconductor can be derived within a mean-field approach originally due to Bogoliubov (Bogoliubov *et al.*, 1959; de Gennes, 1966).

One usually starts with the effective, mean-field Hamiltonian

$$\hat{H} = \int d\mathbf{r} \hat{\psi}^{\dagger}_{\alpha}(\mathbf{r}) \left[\mathcal{H}_0 + U(\mathbf{r})\right] \hat{\psi}_{\alpha}(\mathbf{r}) + \int d\mathbf{r} \left[\Delta(\mathbf{r}) \hat{\psi}^{\dagger}_{\uparrow}(\mathbf{r}) \hat{\psi}^{\dagger}_{\downarrow}(\mathbf{r}) + \text{H.c.}\right] \qquad (17)$$

generalizing the BCS effective Hamiltonian to the inhomogeneous case. Here, $\hat{\psi}^{\dagger}_{\alpha}(\mathbf{r})$ $[\hat{\psi}_{\alpha}(\mathbf{r})]$ is a creation [annihilation] Fermion field operator (with understood summations over repeated spin indices), $\Delta(\mathbf{r})$ is a spatially varying pairing potential, self-consistently taking into account for the electron-electron interaction, which is

here assumed to be described by a spin independent, strongly local potential, as in Eq. (2). In Eq. (17), the kinetic term reads

$$\mathcal{H}_0 = -\frac{\hbar^2}{2m}\left(\nabla - \frac{ie}{\hbar c}\mathbf{A}\right)^2 - \mu, \tag{18}$$

with μ again the chemical potential and $\mathbf{A}(\mathbf{r})$ the electromagnetic vector potential, and $U(\mathbf{r})$ is the self-consistent potential experienced by single particles.

One may conveniently expand the field operators over a complete basis set as

$$\hat{\psi}_\alpha(\mathbf{r}) = \sum_\nu \phi_\nu(\mathbf{r})\hat{c}_{\nu\alpha}, \tag{19}$$

where $\hat{c}_{\nu\alpha}$, $\hat{c}^\dagger_{\nu\alpha}$ obey the usual Fermion anticommutation rules, and $\phi_\nu(\mathbf{r})$ are eigenfunctions of $\mathcal{H}_0$ with eigenvalues ξ_ν (measured from the Fermi level). Depending on the particular symmetry of the problem under study, $\phi_\nu(\mathbf{r})$ may be plane waves, or more complicated functions (see, *e.g.,* Gygi and Schlüter, 1991, for an instance of axially symmetric systems).

Since the effective Hamiltonian, Eq. (17), is quadratic in the field operators, it can be diagonalized by means of a Bogoliubov-Valiatin canonical transformation (Schrieffer, 1964), but now allowing for spatially varying coherent factors $u_\nu(\mathbf{r})$ and $v_\nu(\mathbf{r})$:

$$\hat{\psi}_\uparrow(\mathbf{r}) = \sum_\nu [u_\nu(\mathbf{r})\hat{\gamma}_{\nu\uparrow} - v^*_\nu(\mathbf{r})\hat{\gamma}^\dagger_{\nu\downarrow}] \tag{20a}$$

$$\hat{\psi}_\downarrow(\mathbf{r}) = \sum_\nu [u_\nu(\mathbf{r})\hat{\gamma}_{\nu\downarrow} + v^*_\nu(\mathbf{r})\hat{\gamma}^\dagger_{\nu\uparrow}], \tag{20b}$$

with $\hat{\gamma}^\dagger_{\nu\alpha}$ [$\hat{\gamma}_{\nu\alpha}$] Fermion creation [annihilation] operators for the quasiparticles in the superconducting state.

One then requires that Eqs. (20) diagonalize the effective Hamiltonian, Eq. (17), as

$$\hat{H} = E_0 + \sum_{\nu\alpha} \epsilon_\nu \hat{\gamma}^\dagger_{\nu\alpha}\hat{\gamma}_{\nu\alpha}, \tag{21}$$

where E_0 is the energy of the superconducting ground state. One then easily finds $[\hat{H}, \hat{\gamma}_{\nu\alpha}] = -\epsilon_\nu \hat{\gamma}_{\nu\alpha}$ and $[\hat{H}, \hat{\gamma}^\dagger_{\nu\alpha}] = \epsilon_\nu \hat{\gamma}^\dagger_{\nu\alpha}$. On the other hand, from Eq. (17), one has

$$\left[\hat{H}, \hat{\psi}_\uparrow(\mathbf{r})\right] = -\mathcal{H}\hat{\psi}_\uparrow(\mathbf{r}) - \Delta(\mathbf{r})\hat{\psi}^\dagger_\downarrow(\mathbf{r}) \tag{22a}$$

$$\left[\hat{H}, \hat{\psi}_\downarrow(\mathbf{r})\right] = -\mathcal{H}\hat{\psi}_\downarrow(\mathbf{r}) + \Delta(\mathbf{r})\hat{\psi}^\dagger_\uparrow(\mathbf{r}), \tag{22b}$$

where $\mathcal{H} = \mathcal{H}_0 + U(\mathbf{r})$, and making use of the transformations Eqs. (20) one eventually obtains

$$\epsilon_\nu u_\nu(\mathbf{r}) = \mathcal{H}u_\nu(\mathbf{r}) + \Delta(\mathbf{r})v_\nu(\mathbf{r}) \tag{23a}$$

$$\epsilon_\nu v_\nu(\mathbf{r}) = -\mathcal{H}^* v_\nu(\mathbf{r}) + \Delta^*(\mathbf{r})u_\nu(\mathbf{r}), \tag{23b}$$

which are the static Bogoliubov-de Gennes (BdG) equations (Bogoliubov *et al.*, 1959; de Gennes, 1966).

Eqs. (23) can be written in compact matrix form as an eigenvalue problem for the coherence factors:

$$\begin{pmatrix} \mathcal{H} & \Delta(\mathbf{r}) \\ \Delta^*(\mathbf{r}) & -\mathcal{H}^* \end{pmatrix} \begin{pmatrix} u_\nu(\mathbf{r}) \\ v_\nu(\mathbf{r}) \end{pmatrix} = \epsilon_\nu \begin{pmatrix} u_\nu(\mathbf{r}) \\ v_\nu(\mathbf{r}) \end{pmatrix}. \tag{24}$$

Within such a mean-field approach, the pairing potential $\Delta(\mathbf{r})$ and the single-particle potential $U(\mathbf{r})$ are identified with the self-consistent statistical averages

$$\Delta(\mathbf{r}) = g\langle\hat{\psi}_\downarrow(br)\hat{\psi}_\uparrow(br)\rangle \tag{25a}$$

$$U(\mathbf{r}) = g\langle\hat{\psi}^\dagger_\uparrow(br)\hat{\psi}_\uparrow(br)\rangle, \tag{25b}$$

which, on making use of Eqs. (20), become:

$$\Delta(\mathbf{r}) = -g\sum_\nu v^*_\nu(\mathbf{r})u_\nu(\mathbf{r})(1-2f_\nu) \tag{26a}$$

$$U(\mathbf{r}) = g\sum_\nu \left[|u_\nu(\mathbf{r})|^2 f_\nu + |v_\nu(\mathbf{r})|^2(1-f_\nu)\right], \tag{26b}$$

where $f_\nu = [\exp(\epsilon_\nu/k_{\rm B}T)+1]^{-1}$ is the Fermi function evaluated at ϵ_ν. Thus, superconductivity in an inhomegeneous system is governed by the eigenvalue problem given by the BdG Eqs. (23), and the two self-consistency conditions, Eqs. (26). In analogy with Eq. (6), also the BdG equations can be generalized to the time dependent case.

One possible variational derivation of the BdG equations rests on the generalization of density functional theory (DFT) to superconductors (Oliveira *et al.*, 1988). There, Eqs. (23) can be identified with the Kohn-Sham equations for an appropriate Hohenberg-Kohn functional of both particle density

$$n(\mathbf{r}) = \sum_\sigma \langle\hat{\psi}^\dagger_\sigma(\mathbf{r})\hat{\psi}_\sigma(\mathbf{r})\rangle \tag{27}$$

and the superconducting order parameter

$$\chi(\mathbf{r},\mathbf{r}') = \langle\hat{\psi}_\uparrow(\mathbf{r})\hat{\psi}_\downarrow(\mathbf{r}')\rangle, \tag{28}$$

here generalized to take into account nonlocal effects. Such an approach has been recently employed to evaluate the superconducting condensation energy of the homogeneous electron gas with anisotropic pairing potentials, with angular momentum ℓ ranging from 1 to 9 (Wierzbowska and Krogh, 2005).

6 Integral equation transcending static GP equation taking Bogoliubov-de Gennes theory as starting point

In a very stimulating recent contribution, Pieri and Strinati (2003) (referred to as PS below) have 'derived' the non-linear GP differential equation for condensed bosons by taking as their starting point the Bogoliubov-de Gennes equation for superfluid fermions.

The purpose of this section (see also Angilella *et al.*, 2004) is to demonstrate that one can generalize the zero-temperature differential GP equation while remaining within the original framework of PS, an integral equation formulation then resulting. The framework of PS is provided by the coupled integral equations involving Green functions G_{21}, G_{11} and $\tilde{G}_\circ$. The equations are:

$$G_{11}(\mathbf{r},\mathbf{r}';\omega_s) = \tilde{G}_\circ(\mathbf{r},\mathbf{r}';\omega_s) + \int d\mathbf{r}''\tilde{G}_\circ(\mathbf{r},\mathbf{r}'';\omega_s)\Delta(\mathbf{r}'')G_{21}(\mathbf{r}'',\mathbf{r}';\omega_s), \quad (29a)$$

$$G_{21}(\mathbf{r},\mathbf{r}';\omega_s) = -\int d\mathbf{r}''\tilde{G}_\circ(\mathbf{r}'',\mathbf{r};-\omega_s)\Delta^*(\mathbf{r}'')G_{11}(\mathbf{r}'',\mathbf{r}';\omega_s), \quad (29b)$$

where $\omega_s = (2s+1)\pi/\beta$ (s is an integer) is a fermionic Matsubara frequency, $\beta = 1/k_{\rm B}T$, G_{11} is the normal and G_{21} is the anomalous single-particle Green function. The third Green function appearing in Eqs. (29), namely $\tilde{G}_\circ$, satisfies the equation

$$[i\omega_s - H(\mathbf{r})]\tilde{G}_\circ(\mathbf{r},\mathbf{r}';\omega_s) = \delta(\mathbf{r}-\mathbf{r}'), \quad (30)$$

where the single-particle Hamiltonian $H(\mathbf{r})$ is defined by:

$$H(\mathbf{r}) = -\frac{1}{2m}\nabla^2 + V(\mathbf{r}) - \mu, \quad (31)$$

μ being the Fermionic chemical potential. As PS stress, Eqs. (29), when taken together with the self-consistency equation for the gap function:

$$\Delta^*(\mathbf{r}) = \frac{V_0}{\beta}\sum_s G_{21}(\mathbf{r},\mathbf{r};\omega_s), \quad (32)$$

are entirely equivalent to the Bogoliubov-de Gennes equations that describe the behavior of superfluid fermions in the presence of an external potential. Equations (29–32) define what we have termed the original framework of the PS study. The constant $V_0 < 0$ entering Eq. (32) arises from the contact potential $V_0\delta(\mathbf{r}-\mathbf{r}')$ assumed by PS to act between fermions with opposite spins. We also retain here their use of the ratio $\Delta(\mathbf{r})/\mu$ as an expansion parameter which allows the rapid truncation of such series, which then leads for strong coupling to an integral equation for the gap function

$$-\frac{1}{V_0}\Delta^*(\mathbf{r}) = \int d\mathbf{r}_1\, Q(\mathbf{r},\mathbf{r}_1)\Delta^*(\mathbf{r}_1) + \int d\mathbf{r}_1 d\mathbf{r}_2 d\mathbf{r}_3\, R(\mathbf{r},\mathbf{r}_1,\mathbf{r}_2,\mathbf{r}_3)\Delta^*(\mathbf{r}_1)\Delta(\mathbf{r}_2)\Delta^*(\mathbf{r}_3), \quad (33)$$

where R is written explicitly in terms of $\tilde{G}_\circ(\mathbf{r}, \mathbf{r}_1; \omega_s)$ in Eq. (15) of PS. However, as will emerge below, it is the non-local kernel $Q(\mathbf{r}, \mathbf{r}')$ which is at the heart of the present study. In terms of the Green function $\tilde{G}_\circ$ entering Eq. (30), $Q(\mathbf{r}, \mathbf{r}')$ is given by [PS: Eq. (14)]:

$$Q(\mathbf{r}, \mathbf{r}') = \frac{1}{\beta} \sum_s \tilde{G}_\circ(\mathbf{r}', \mathbf{r}; -\omega_s) \tilde{G}_\circ(\mathbf{r}', \mathbf{r}; \omega_s). \tag{34}$$

We take the integral equation (33) for the gap function as the starting point of this section. For our purposes below, it is then crucial to gain insight into the kernel Q in Eq. (34), and in particular to carry out the summation explicitly over the Matsubara frequencies ω_s.

To gain orientation, let us first perform this summation when the external potential $V(\mathbf{r})$ is set to zero in Eq. (30). Having achieved this summation, we shall present a general method to allow the sum over ω_s to be achieved for $V(\mathbf{r}) \neq 0$, using earlier work of Stoddart *et al.* (1968).

Returning to the explicit form of $Q(\mathbf{r}, \mathbf{r}_1)$ given in Eq. (34) above, it is natural to study first the translational invariant, free-electron limit of Eq. (34), say $Q_\circ(r)$, with $r = |\mathbf{r} - \mathbf{r}_1|$, which is obtained by 'switching off' the one-body potential $V(\mathbf{r})$. This amounts to replacing $\tilde{G}_\circ$ in Eq. (34) with the free-electron Green function $G_\circ$. For the Fourier transform of $Q_\circ(r)$, we formally find

$$\hat{Q}_\circ(k) = \int \frac{d\mathbf{k}'}{(2\pi)^3} \frac{1 - n_{\mathrm{F}}(\xi_{\mathbf{k}-\mathbf{k}'}) - n_{\mathrm{F}}(\xi_{\mathbf{k}'})}{\xi_{\mathbf{k}-\mathbf{k}'} + \xi_{\mathbf{k}'}}, \tag{35}$$

where $\xi_{\mathbf{k}} = k^2/2m - \mu$ and $n_{\mathrm{F}}(\xi)$ is the Fermi-Dirac distribution function. However, it should be noted that, in three dimensions, Eq. (35) contains a divergent contribution at large wave-numbers, which implies a divergent behavior of $Q_\circ(r)$ at small distances r. Indeed, we find the asymptotic expansion (see also Alexandrov, 2003):

$$\frac{4\mu}{k_{\mathrm{F}}^6} Q_\circ(r) \sim \frac{1}{4\pi^2} \frac{1}{r'^2 \beta'} \frac{1}{\sinh a}, \quad \beta' \gg 1, \tag{36}$$

where $r' = k_{\mathrm{F}} r$, k_{F} is the Fermi wave-number, defined by $\mu = k_{\mathrm{F}}^2/2m$, $\beta' = \beta\mu$, and $a = r'\pi/\beta'$. Fig. 12 shows then our numerical results for $r'^4 Q_\circ(r')$, as a function of r', for several temperatures ($\beta' = 10 - 30$).

Following Stoddart *et al.* (1968), the canonical density matrix $C(\mathbf{r}, \mathbf{r}', \beta)$ is defined by

$$C(\mathbf{r}, \mathbf{r}', \beta) = \sum_i \psi_i(\mathbf{r}) \psi_i^*(\mathbf{r}') e^{-\beta\epsilon_i}, \tag{37}$$

where $\beta = 1/k_{\mathrm{B}}T$. Within the perturbative approach of March and Murray (1960, 1961), with plane waves as the unperturbed solution, the canonical density matrix can then be written to all orders in the external potential $V(\mathbf{r})$ in terms of the free-particle canonical density matrix given by

$$C_0(z, \beta) = (2\pi\beta)^{-3/2} \exp(-z^2/2\beta), \tag{38}$$

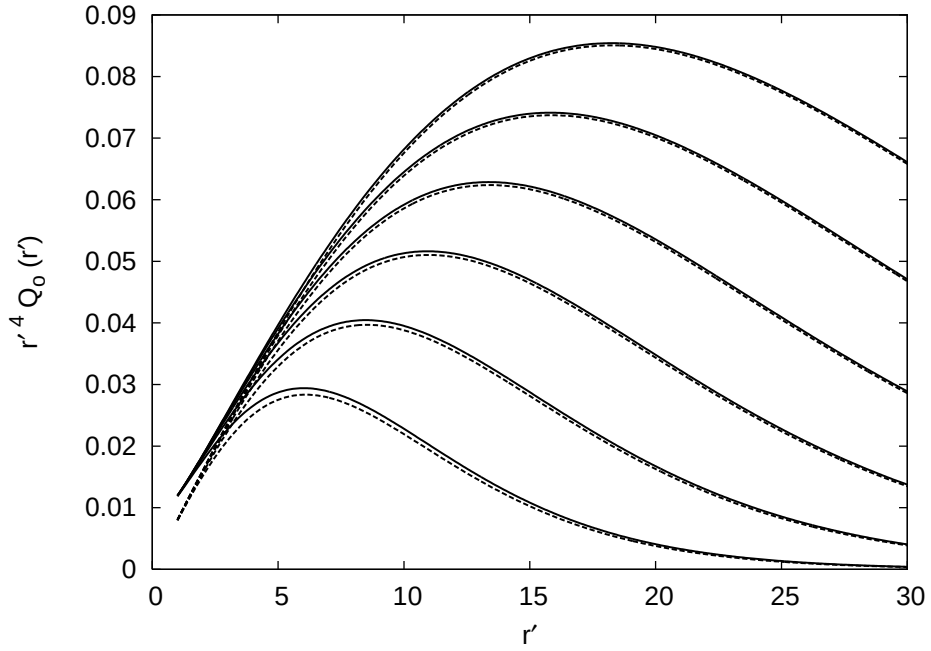

Figure 12: Solid lines show $r'^4 Q_\circ(r')$, where $Q(r)$ is defined by Eq. (34), as a function of $r' = k_{\rm F} r$, for several temperatures, given by $\beta' = \beta\mu = 10 - 30$ (bottom to top). Dashed lines are the asymptotic expansion Eq. (36). Units are such that $k_{\rm F}^6/(4\mu) = 1$. Redrawn from Angilella *et al.* (2004).

as

$$C(\mathbf{r}, \mathbf{r}_0, \beta) = \int_0^\infty dz\, z\, C_0(z, \beta) f(z, \mathbf{r}, \mathbf{r}_0), \tag{39}$$

where f satisfies the integral equation (Stoddart *et al.*, 1968):

$$f(z, \mathbf{r}, \mathbf{r}_0) = \frac{1}{z}\delta(z - |\mathbf{r} - \mathbf{r}_0|) - \int d\mathbf{r}_1 \frac{V(\mathbf{r}_1)}{2\pi|\mathbf{r} - \mathbf{r}_1|} f(z - |\mathbf{r} - \mathbf{r}_1|, \mathbf{r}_1, \mathbf{r}_0). \tag{40}$$

The desired Green function $\tilde{G}_\circ$ is then to be obtained from f entering Eqs. (39) and (40) as (Stoddart *et al.*, 1968)

$$\tilde{G}_\circ(\mathbf{r}, \mathbf{r}_1; k) = \int_0^\infty dz\, z\, \bar{G}_\circ(z; k) f(z, \mathbf{r}, \mathbf{r}_1), \tag{41}$$

where

$$\bar{G}_\circ(z; k) = \frac{e^{ikz}}{4\pi z}. \tag{42}$$

One may also take advantage of the expression in Eq. (41) of $\tilde{G}_\circ$ in terms of $\bar{G}_\circ$ to rewrite the kernel $Q(\mathbf{r}, \mathbf{r}_1)$ defined by Eq. (34) as

$$Q(\mathbf{r}, \mathbf{r}_1) = \int_0^\infty dz_1\, dz_2\, z_1\, z_2\, f(z_1, \mathbf{r}_1, \mathbf{r}) f(z_2, \mathbf{r}_1, \mathbf{r}) Q_\circ(z_1, z_2), \tag{43}$$

where the Fourier transform of $Q_\circ(z_1, z_2)$ is given by

$$\hat{Q}_\circ(\mathbf{k}_1, \mathbf{k}_2) = \frac{1 - n_{\rm F}(\xi_{\mathbf{k}_1}) - n_{\rm F}(\xi_{\mathbf{k}_2})}{\xi_{\mathbf{k}_1} + \xi_{\mathbf{k}_2}}. \tag{44}$$

Hence, the sum over Matsubara frequencies has still been carried out in the presence of an external potential $V(\mathbf{r})$ entering Eq. (40) for the function f.

Because of current interest in harmonic confinement in magnetic traps at low temperatures, let us illustrate the rather formal Eqs. (39) and (40) when the external potential $V(\mathbf{r})$ has the explicit isotropic harmonic oscillator form in three dimensions, namely

$$V(\mathbf{r}) = \frac{1}{2} m\omega^2 r^2. \tag{45}$$

Following the pioneering work of Sondheimer and Wilson (1951) on free electrons in a magnetic field, the diagonal element $C(\mathbf{r}, \mathbf{r}, \beta)$ when $V(\mathbf{r})$ is given by Eq. (45) takes the form (see *e.g.* March *et al.*, 1995, p. 27; see also Howard *et al.*, 2003)

$$C(\mathbf{r}, \mathbf{r}, \beta) = \left(\frac{m}{2\pi\hbar}\right)^{3/2} \left(\frac{\omega}{\sinh \hbar\omega\beta}\right)^{3/2} \exp\left(-\frac{m}{\hbar}\omega r^2 \tanh \frac{1}{2}\hbar\omega\beta\right), \tag{46}$$

which is the so-called Slater sum of quantum chemistry (Fig. 13).

From Eqs. (38) and (39), performing the substitution $t = z^2/2$, it then follows that $f(z, \mathbf{r}, \mathbf{r}_0)$ can be expressed as the inverse Laplace transform

$$f(z, \mathbf{r}, \mathbf{r}_0) = (2\pi)^{3/2} \mathcal{L}^{-1}\left[s^{-3/2} C(\mathbf{r}, \mathbf{r}_0, s^{-1})\right] \tag{47}$$

where (t, s) are conjugate variables with respect to the Laplace transform.

Within the Thomas-Fermi (TF) approximation, we take:

$$C_{\rm TF}(\mathbf{r}, \mathbf{r}, \beta) = \frac{1}{(2\pi\beta)^{3/2}} \exp[-\beta V(\mathbf{r})], \tag{48}$$

which is plotted also in Fig. 13 for $V(\mathbf{r})$ given by Eq. (45). For the value of β shown, the TF form Eq. (48) is seen to be a useful approximation to the exact result, Eq. (46). Inserting Eq. (48) into Eq. (47) we find

$$f_{\rm TF}(z, \mathbf{r}, \mathbf{r}) = \frac{\delta(z)}{z} - \frac{\sqrt{2V(\mathbf{r})}}{z} J_1[\sqrt{2V(\mathbf{r})} z], \tag{49}$$

where J_1 denotes the Bessel function of the first kind and order one.

Fig. 14 shows $f(z, \mathbf{r}, \mathbf{r})$ as a function of r for fixed z, as obtained by numerically performing the inverse Laplace transform in Eq. (47) for the harmonic potential case. The regular contribution to the analytic result for the Thomas-Fermi approximation, Eq. (49), is also plotted for comparison. The similarity in shape between approximate and (numerically) exact results for this harmonic confinement model

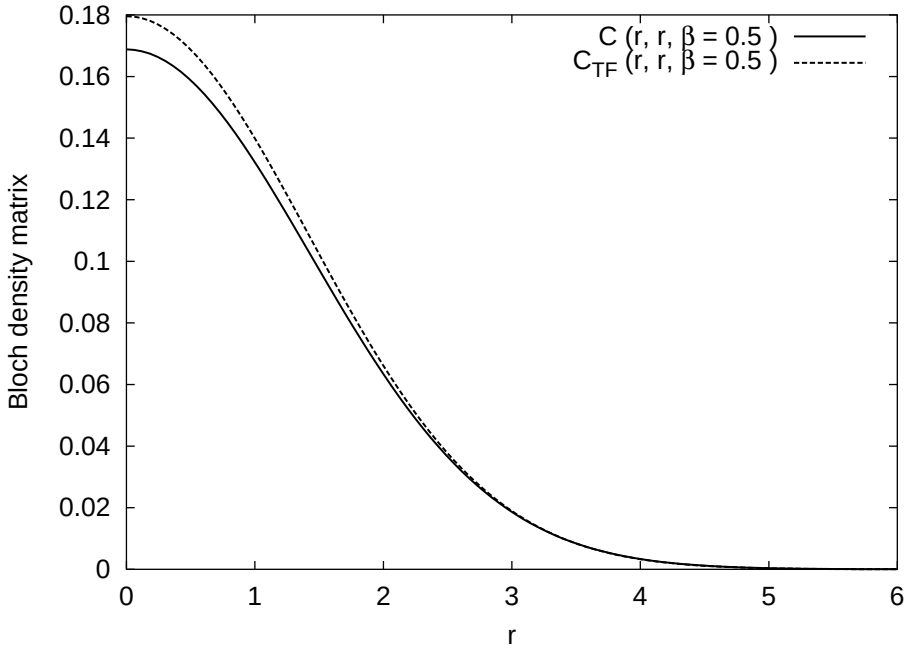

Figure 13: Shows diagonal element of the canonical density matrix $C(\mathbf{r},\mathbf{r},\beta)$, Eq. (46), and its Thomas-Fermi approximation, Eq. (48), as a function of r, for $\beta = 0.5$. Energies are in units of $\hbar\omega$, while lengths are in units of $(\hbar/m\omega)^{1/2}$. Redrawn from Angilella *et al.* (2004).

seems to us rather remarkable. After this model test of a TF-like approximation invoked by PS, we return to the general case, based on the exact result Eq. (43) for the kernel $Q(\mathbf{r},\mathbf{r}_1)$.

Then, we invert the argument of PS but still use a further essential assumption of their study, namely that the condensate wave function $\Phi(\mathbf{r})$ entering the Gross-Pitaevskii equation is related to the gap function $\Delta(\mathbf{r})$ by

$$\Phi(\mathbf{r}) = \left(\frac{m^2 a_{\rm F}}{8\pi}\right)^{1/2} \Delta(\mathbf{r}) \equiv k\Delta(\mathbf{r}). \tag{50}$$

Here, in the strong coupling limit, and following PS, $a_{\rm F} \sim (2m|\mu|)^{-1/2}$ represents the characteristic length scale for the non-interacting Green function $G_\circ$, equal to $\tilde{G}_\circ$ above when $V(\mathbf{r})$ is put equal to zero.

Given the validity of this PS assumption, Eq. (50), we then rewrite Eq. (33) as an equation for $\Phi(\mathbf{r})$:

$$\begin{aligned} -\frac{1}{V_0}\Phi^*(\mathbf{r}) &= \int d\mathbf{r}_1\, Q(\mathbf{r},\mathbf{r}_1)\Phi^*(\mathbf{r}_1) \\ &\quad + \frac{1}{k^2}\int d\mathbf{r}_1 d\mathbf{r}_2 d\mathbf{r}_3\, R(\mathbf{r},\mathbf{r}_1,\mathbf{r}_2,\mathbf{r}_3)\Phi^*(\mathbf{r}_1)\Phi(\mathbf{r}_2)\Phi^*(\mathbf{r}_3). \end{aligned} \tag{51}$$

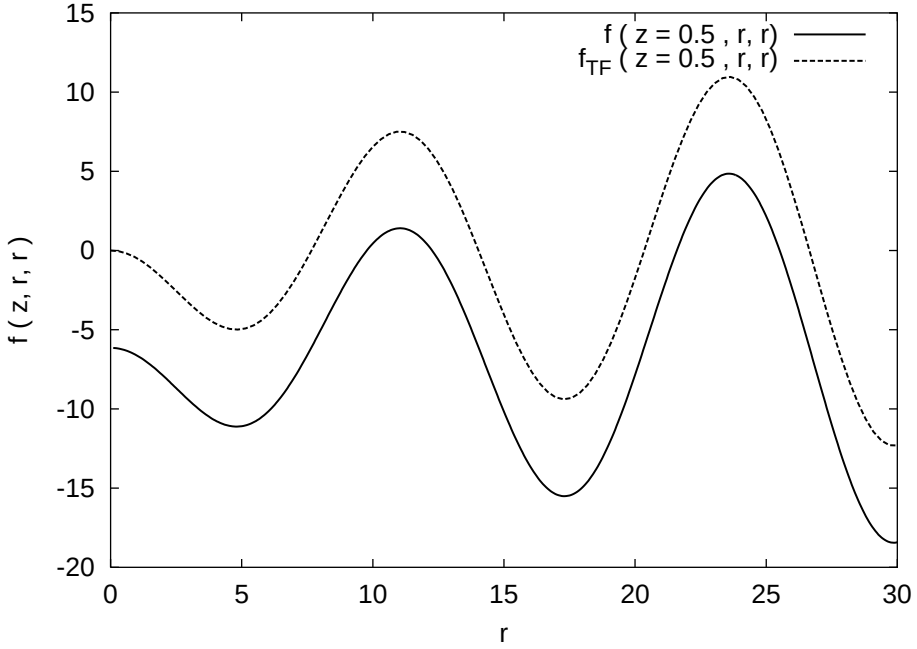

Figure 14: Shows diagonal $f(z, \mathbf{r}, \mathbf{r})$ corresponding to the harmonic potential, as given by the inverse Laplace transform, Eq. (47), as well as the regular part of its Thomas-Fermi approximation, Eq. (49), as a function of r, for fixed $z = 0.5$. Units as in Fig. 13. Redrawn from Angilella *et al.* (2004).

This then is the proposed generalization of the Gross-Pitaevskii equation, but with $Q(\mathbf{r}, \mathbf{r}_1)$ to be calculated more accurately than by the Thomas-Fermi–like assumption of Pieri and Strinati (2003), via Eqs. (43) and (40).

While Eq. (51) is a direct consequence of the above arguments, it remains an expansion in Φ, in suitable reduced form. Therefore, a first attempt to simplify this Eq. (51) is to retain the approximation given by the Pieri-Strinati approach in the 'smallest' term involving $O(\Phi^3)$ on the right-hand side of the basic Eq. (51). Thus one reaches the (still non-local) equation for the condensate wave function $\Phi(\mathbf{r})$:

$$-\frac{1}{V_0}\Phi^*(\mathbf{r}) = \int d\mathbf{r}_1\, Q(\mathbf{r}, \mathbf{r}_1)\Phi(\mathbf{r}_1) - \frac{1}{2} m a_{\mathrm{F}}^2 |\Phi(\mathbf{r})|^2 \Phi(\mathbf{r}). \tag{52}$$

For sufficiently small spatial variations in the condensate wave function $\Phi(\mathbf{r})$ in Eq. (52), the basic nonlocality can be removed by Taylor expanding $\Phi(\mathbf{r}_1)$ around the position $\mathbf{r}$ in the integral term. This then characterizes the problem in terms of 'partial moments' of the kernel $Q(\mathbf{r}, \mathbf{r}_1)$, namely $\int Q(\mathbf{r}, \mathbf{r}_1) d\mathbf{r}_1$ and $\int Q(\mathbf{r}, \mathbf{r}_1) |\mathbf{r} - \mathbf{r}_1|^2 d\mathbf{r}_1$. Such partial moments then enter the original GP equation, as stressed by PS.

In summary, we propose the retention of the non-local kernel $Q(\mathbf{r}, \mathbf{r}_1)$ as in

Eq. (51) above, since the sum over Matsubara frequencies in Eq. (34) has been performed in Eq. (43), which is a central result of the present study. However, in the terms of $O(\Phi^3)$ in Eq. (51), a sensible starting point is to follow the PS approximation displayed in Eq. (52).

As to future directions, evaluation of the non-local kernel in Eq. (43) for other external potentials than the harmonic case in Eq. (45) is of obvious interest. For this latter model, though our Fig. 14 considers the diagonal element of $f(z, \mathbf{r}, \mathbf{r}_1)$, the off-diagonal form of $C(\mathbf{r}, \mathbf{r}_1, \beta)$ is known (Howard *et al.*, 2003), and numerical Laplace inversion to obtain $f(z, \mathbf{r}, \mathbf{r}_1)$ is entirely feasible. Then $Q(\mathbf{r}, \mathbf{r}_1)$ can be obtained, though of course numerically.

The GP equation is valid in the strong-coupling limit of superfluidity. It has to be stressed that in the weak coupling limit one can also derive a Ginzburg-Landau equation starting from the Bogoliubov-de Gennes equations. We note specifically in this context that the derivation of the Ginzburg-Landau equation in the weak-coupling limit for the harmonic trap was presented by Baranov and Petrov (1998). The results presented in this section are also relevant to the weak-coupling limit of superfluidity.

Finally, we return to the foundations of the Gross-Pitaevskii equation by Leggett (2003), which we summarized very briefly in Section 4 above. Leggett concludes that there is no correlated many-body wave-function underlying their original equation. It will be interesting for the future to know whether the non-local versions of Eqs. (51) and (52) proposed here are still subject to this limitation.

7 Summary and suggestions for further study

In summary, the GP Eqs. (4) and (6) have been considered in relation to a variety of experiments on inhomogeneous condensed Bosons in Sections 2 first and, predominantly, in Section 3.

Sections 4–6 are then theoretical in emphasis. The short Section 4 summarizes the arguments of Leggett (2003), which reveal that there is no underlying many-body wave function for the static GP Eq. (4). Therefore, instead of the GP differential equation, Sections 5 and 6 present an integral equation theory (Angilella *et al.*, 2004) for which the starting point is the Bogoliubov-de Gennes theory.

7.1 Suggestions for further study

Though a non-local theory given in Section 6, in the form of an integral equation, trascends the static GP differential Eq. (4), no proof has, as yet, been given that this integral equation theory has, underlying it, a many-body wave function. It seems that this, therefore, in view of Leggett's criticism of the foundations of the static GP Eq. (4), is an area of considerable interest for further theoretical work.

O'Dell *et al.* (2004) have developed, within the Thomas-Fermi regime, the hydrodynamics of a trapped dipolar BEC. As they stress, such a BEC, whose particles interact via dipole-dipole coupling, constitute an example of a superfluid with long-range and anisotropic interparticle forces. This contrasts with the customary BECs which are characterized by isotropic interactions with range much smaller than the average interparticle interaction (see *e.g.* Dalfovo *et al.*, 1999). While alkali atoms have small dipole-dipole interactions, O'Dell *et al.* suggest that chromium is a promising case for a dipolar BEC, due to its large magnetic moment of 6 Bohr magnetons, and there has been progress in cooling it towards degeneracy (Schmidt *et al.*, 2003; Hensler *et al.*, 2003). As O'Dell *et al.* also note, molecules can possess large dipole moments. They suggest that advances in the cooling of polar molecules (Weinstein *et al.*, 1998; Bethlem *et al.*, 1999, 2000, 2002), photoassociation of ultracold heteronuclear molecules (Mancini *et al.*, 2004), and molecular BECs (Greiner *et al.*, 2003; Jochim *et al.*, 2003; Zwierlein *et al.*, 2003) may soon lead to superfluids where dipolar effects play a major role.

O'Dell *et al.* (2004) consider in their Letter a harmonically trapped BEC with dipole-dipole interactions as well as short-range s-wave scattering. They note that in the Thomas-Fermi limit, where the zero-point kinetic energy of the atoms in the trap can be neglected compared with the interparticle interaction energy and the trapping potential, the collective dynamics of a BEC may be treated by the collisionless hydrodynamic theory of Bose superfluids at $T = 0$ (Stringari, 1996). The effect of the dipolar interactions is to introduce non-locality into the already nonlinear hydrodynamic equations.

In relation to the focus of the present review on the GP equations, it is to be emphasized (O'Dell *et al.*, 2004) that the dominant interactions in the ultracold gases available at the time of writing are asymptotically of van der Waals character, with an r^{-6} decay, and are short-ranged, compared with the mean interactomic distance. As we have seen above, within the mean-field regime of the GP equations these interactions are represented by the pseudopotential model $g\delta(\mathbf{r}) \equiv (4\pi a_s\hbar^2/m)\delta(\mathbf{r})$ [cf. Eqs. (2) and (3)]. By employing a Fano-Feshbach resonance, it is possible to adjust the value of a_s to yield repulsive (positive) and attractive (negative) values (Inouye *et al.*, 1998). Appealing to the analogy of nuclear magnetic resonance techniques, dipole-dipole interactions can also be controlled by rapidly rotating an external field (Giovanazzi *et al.*, 2002). The interactions vanish when the rotation corresponds to the so-called magic angle.

To summarize here the main points made by O'Dell *et al.* (2004), the versatility of quantum gases is promising for the study of the role of interactions in superfluidity. They present solutions of the dipolar superfluid hydrodynamic equations in a harmonic trap: the condensate density is parabolic as in the pure s-wave problem but now with modified radii.

Finally, and returning to the Fano-Feshbach resonances already referred to (Fano, 1935; Feshbach, 1958), there remains the important question for theory of the

crossover of Bosonic to Fermionic superfluidity (see, *e.g.,* Randeria, 1995), following, for example, the pioneering studies of Nozières and Schmitt-Rink (1985) (see also Timmermans *et al.*, 2001). Note that the cold-atom technology that has resulted in the observation of dilute-gas BECs enables the creation and subsequent studies of physical properties of novel superfluids having a degree of flexibility adding to the already powerful methods of traditional low temperature physics. This therefore seems a further, and very attractive, direction for further studies.

Acknowledgements

The authors would like to thank N. Andrenacci, M. Baldo, M. L. Chiofalo, I. A. Howard, M. Inguscio, E. Rimini, and M. P. Tosi for useful discussions on the general area embraced by the present review.

References

Alexandrov, A. S., *Theory of superconductivity: From Weak to Strong Coupling* (IOP, Bristol, 2003).

Anderson, B. P. and Kasevich, M. A., (1998). Science **281**, 1686.

Andrews, M. R., Townsend, C. G., Miesner, H. J., Durfee, D. S., Kurn, D. M., and Ketterle, W., (1997). Science **275**, 637.

Angilella, G. G. N., March, N. H., and Pucci, R., (2004). Phys. Rev. A **69**, 055601.

Baranov, M. A. and Petrov, D. S., (1998). Phys. Rev. A **58**, R801.

Barone, A., (2000). Weakly coupled macroscopic quantum systems: likeness with difference. In *Quantum Mesoscopic Phenomena and Mesoscopic Devices in Microelectronics*, edited by Kulik, I. O. and Ellialtioglu, R., volume 559 of *NATO Science Series: C Mathematical and Physical Sciences*, p. 301 (Kluwer, Dordrecht, 2000).

Barone, A. and Paterno, G., *Physics and Applications of the Josephson Effect* (J. Wiley & Sons, New York, 1982).

Bethlem, H. L., Berden, G., Crompvoets, F. M. H., Jongma, R. T., van Roij, A. J. A., and Meijer, G., (2000). Nature (London) **406**, 491.

Bethlem, H. L., Berden, G., and Meijer, G., (1999). Phys. Rev. Lett. **83**, 1558.

Bethlem, H. L., Crompvoets, F. M. H., Jongma, R. T., van de Meerakker, S. Y. T., and Meijer, G., (2002). Phys. Rev. A **65**, 053416.

Bloch, I., Hänsch, T. W., and Esslinger, T., (1999). Phys. Rev. Lett. **82**, 3008.

Bogoliubov, N. N., (1947). J. Phys. (Moscow) **11**, 23.

Bogoliubov, N. N., Tolmachev, V. V., and Shirkov, D. V., *A New Method of Superconductivity* (Consultants Bureau, New York, 1959).

Bongs, K., Burger, S., Birkl, G., Sengstock, K., Ertmer, W., Rzazewski, K., Sanpera, A., and Lewenstein, M., (1999). Phys. Rev. Lett. **83**, 3577.

Bongs, K., Burger, S., Dettmer, S., Hellweg, D., Arlt, J., Ertmer, W., and Sengstock, K., (2001a). Cr. Acad. Scie. IV-Phys. **2**, 671.

Bongs, K., Burger, S., Dettmer, S., Hellweg, D., Arlt, J., Ertmer, W., and Sengstock, K., (2001b). Phys. Rev. A **63**, 031602(R).

Burger, S., Bongs, K., Dettmer, S., Ertmer, W., Sengstock, K., Sanpera, A., Shlyapnikov, G. V., and Lewenstein, M., (1999). Phys. Rev. Lett. **83**, 5198.

Burger, S., Cataliotti, F. S., Fort, C., Maddaloni, P., Minardi, F., and Inguscio, M., (2002). Europhys. Lett. **57**, 1.

Burger, S., Cataliotti, F. S., Fort, C., Minardi, F., Inguscio, M., Chiofalo, M. L., and Tosi, M. P., (2001). Phys. Rev. Lett. **86**, 4447.

Castin, Y. and Dum, R., (1999). Eur. Phys. J. D **7**, 399.

Cataliotti, F. S., Burger, S., Fort, C., Maddaloni, P., Minardi, F., Trombettoni, A., Smerzi, A., and Inguscio, M., (2001). Science **293**, 843.

Cherny, A. Y. and Brand, J., (2004). Phys. Rev. A **70**, 043622.

Chiofalo, M. L., Succi, S., and Tosi, M. P., (1999). Phys. Lett. A **260**, 86.

Chiofalo, M. L. and Tosi, M. P., (2001). Europhys. Lett. **56**, 326.

Chu, S., (1998). Rev. Mod. Phys. **70**, 685.

Cohen-Tannoudji, C. N., (1998). Rev. Mod. Phys. **70**, 707.

Dalfovo, F., Giorgini, S., Pitaevskii, L. P., and Stringari, S., (1999). Rev. Mod. Phys. **71**, 463.

de Gennes, P. G., *Superconductivity of Metals and Alloys* (W. A. Benjamin, New York, 1966).

DeMarco, B., Bohn, J. L., Burke, Jr., J. P., Holland, M., and Jin, D. S., (1998). Phys. Rev. Lett. **82**, 4208.

DeMarco, B. and Jin, D. S., (1999). Science **285**, 1703.

Deng, L., Hagley, E. W., Wen, J., Trippenbach, M., Band, Y., Julienne, P. S., Simsarian, J. E., Helmerson, K., Rolston, S. L., and Phillips, W. D., (1999). Nature (London) **398**, 218.

Denschlag, J., Simsarian, J. E., Feder, D. L., Clark, C. W., Collins, L. A., Cubizolles, J., Deng, L., Hagley, E. W., Helmerson, K., Reinhardt, W. P., Rolston, S. L., Schneider, B. I., and Phillips, W. D., (2000). Science **287**, 97.

Denschlag, J. H., Simsarian, J. E., Haffner, H., McKenzie, C., Browaeys, A., Cho, D., Helmerson, K., Rolston, S. L., and Phillips, W. D., (2002). J. Phys. B: At. Mol. Opt. Phys. **35**, 3095.

Eiermann, B., Treutlein, P., Anker, T., Albiez, M., Taglieber, M., Marzlin, K., and Oberthaler, M. K., (2003). Phys. Rev. Lett. **91**, 060402.

Esteve, J., Aussibal, C., Schumm, T., Figl, C., Mailly, D., Bouchoule, I., Westbrook, C., and Aspect, A., (2004). Phys. Rev. A **70**, 043629.

Fallani, L., Cataliotti, F. S., Catani, J., Fort, C., Modugno, M., Zawada, M., and Inguscio, M., (2003). Phys. Rev. Lett. **91**, 240405.

Fano, U., (1935). Nuovo Cimento **12**, 156.

Fazio, R. and van der Zant, H., (2001). Phys. Rep. **355**, 235.

Feshbach, H., (1958). Ann. Phys. (N.Y.) **5**, 357.

Folman, R., Krüger, P., Cassettari, D., Hessmo, B., Maier, T., and Schmiedmayer, J., (2000). Phys. Rev. Lett. **84**, 4749.

Fort, C., Maddaloni, P., Minardi, F., Modugno, M., and Inguscio, M., (2001). Optics Lett. **26**, 1039.

Fort, C., Prevedelli, M., Minardi, F., Cataliotti, F. S., Ricci, L., Tino, G. M., and Inguscio, M., (2000). Europhys. Lett. **49**, 8.

Fortágh, J., Ott, H., Kraft, S., Günther, A., and Zimmermann, C., (2002). Phys. Rev. A **66**, 041604(R).

García-Ripoll, J. J. and Pérez-García, V. M., (2001). Phys. Rev. A **63**, 041603.

Giovanazzi, S., Görlitz, A., and Pfau, T., (2002). Phys. Rev. Lett. **89**, 130401.

Greiner, M., Mandel, O., Esslinger, T., Hänsch, T. W., and Bloch, I., (2002a). Nature (London) **415**, 39.

Greiner, M., Mandel, O., Hänsch, T. W., and Bloch, I., (2002b). Nature (London) **419**, 51.

Greiner, M., Regal, C. A., and Jin, D. S., (2003). Nature (London) **426**, 537.

Gross, E. P., (1961). Nuovo Cimento **20**, 454.

Gross, E. P., (1963). J. Math. Phys. **4**, 195.

Gygi, F. and Schlüter, M., (1991). Phys. Rev. B **43**, 7609.

Hadzibabic, Z., Stan, C. A., Dieckmann, K., Gupta, S., Zwierlein, M. W., Görlitz, A., and Ketterle, W., (2002). Phys. Rev. Lett. **88**, 160401.

Hänsel, W., Hommelhoff, P., Hänsch, T. W., and Reichel, J., (2001a). Nature (London) **413**, 498.

Hänsel, W., Reichel, J., Hommelhoff, P., and Hänsch, T. W., (2001b). Phys. Rev. Lett. **86**, 608.

Hänsel, W., Reichel, J., Hommelhoff, P., and Hänsch, T. W., (2001c). Phys. Rev. A **64**, 063607.

Harber, D. M., McGuirk, J. M., Obrecht, J. M., and Cornell, E. A., (2003). J. Low Temp. Phys. **133**, 229.

Hensler, S., Werner, J., Griesmaier, A., Schmidt, P. O., Görlitz, A., Pfau, T., Giovanazzi, S., and Rzążewski, K., (2003). Appl. Phys. B **77**, 765.

Hilligsøe, K. M., Oberthaler, M. K., and Marzlin, K., (2002). Phys. Rev. A **66**, 063605.

Howard, I. A., Komarov, I. V., March, N. H., and Nieto, L. M., (2003). J. Phys. A: Math. Gen. **36**, 4757.

Inguscio, M., (2003). Science **300**, 1671.

Inguscio, M., Stringari, S., and Wieman, C. E., editors. *Proceedings of the CXL International School of Physics "E. Fermi" on "Bose-Einstein Condensation in Atomic Gases"* (IOS, Amsterdam, 1998).

Inouye, S., Andrews, M. R., Stenger, J., Miesner, H., D. M. Stamper-Kurn, and Ketterle, W., (1998). Nature (London) **392**, 151.

Inouye, S., Pfau, T., Gupta, S., Chikkatur, A. P., Gorlitz, A., Pritchard, D. E., and Ketterle, W., (1999). Nature (London) **402**, 641.

Jaksch, D., Bruder, C., Cirac, J. I., Gardiner, C. W., and Zoller, P., (1998). Phys. Rev. Lett. **81**, 3108.

Jochim, S., Bartenstein, M., Altmeyer, A., Hendl, G., Riedl, S., Chin, C., Hecker Denschlag, J., and Grimm, R., (2003). Science **302**, 2101.

Jones, M. P. A., Vale, C. J., Sahagun, D., Hall, B. V., and Hinds, E. A., (2003). Phys. Rev. Lett. **91**, 080401.

Jones, W. and March, N. H., *Theoretical Solid-State Physics. Perfect Lattices in Equilibrium*, volume 1 (Dover, London, 1986).

Khaykovich, L., Schreck, F., Ferrari, G., Bourdel, T., Cubizolles, J., Carr, L. D., Castin, Y., and Salomon, C., (2002). Science **296**, 1290.

Konotop, V. V. and Salerno, M., (2002). Phys. Rev. A **65**, 021602.

Kozuma, M., Suzuki, Y., Torii, Y., Sugiura, T., Kuga, T., Hagley, E. W., and Deng, L., (1999). Science **286**, 2309.

Leggett, A. J., (2001). Rev. Mod. Phys. **73**, 307.

Leggett, A. J., (2003). New J. Phys. **5**, 103.1.

Lenz, G., Meystre, P., and Wright, E. M., (1994). Phys. Rev. A **50**, 1681.

Lieb, E. H. and Yngvason, J., (1998). Phys. Rev. Lett. **80**, 2504.

Lin, Y., Teper, I., Chin, C., and Vuletić, V., (2004). Phys. Rev. Lett. **92**, 050404.

Makhlin, Y., Schön, G., and Shnirman, A., (2001). Rev. Mod. Phys. **73**, 357.

Mancini, M. W., Telles, G. D., Caires, A. R. L., Bagnato, V. S., and Marcassa, L. G., (2004). Phys. Rev. Lett. **92**, 133203.

Mandel, O., Greiner, M., Widera, A., Rom, T., Hänsch, T. W., and Bloch, I., (2003). Nature (London) **425**, 937.

March, N. H. and Murray, A. M., (1960). Phys. Rev. **120**, 830.

March, N. H. and Murray, A. M., (1961). Proc. Roy. Soc. A **261**, 119.

March, N. H., Young, W. H., and Sampanthar, S., *The Many-Body Problem in Quantum Mechanics* (Dover, New York, 1995).

Massignan, P. and Modugno, M., (2003). Phys. Rev. A **67**, 023614.

Mewes, M., Andrews, M. R., Kurn, D. M., Durfee, D. S., Townsend, C. G., and Ketterle, W., (1997). Phys. Rev. Lett. **78**, 582.

Minguzzi, A., Succi, S., Toschi, F., Tosi, M. P., and Vignolo, P., (2004). Phys. Rep. **395**, 223.

Nozières, P. and Schmitt-Rink, S., (1985). J. Low Temp. Phys. **59**, 195.

O'Dell, D. H. J., Giovanazzi, S., and Eberlein, C., (2004). Phys. Rev. Lett. **92**, 250401.

Oliveira, L. N., Gross, E. K. U., and Kohn, W., (1988). Phys. Rev. Lett. **60**, 2430.

Ott, H., Fortagh, J., Schlotterbeck, G., Grossmann, A., and Zimmermann, C., (2001). Phys. Rev. Lett. **87**, 230401.

Paredes, B., Widera, A., Murg, V., Mandel, O., Fölling, S., Cirac, I., Shlyapnikov, G. V., Hänsch, T. W., and Bloch, I., (2004). Nature (London) **429**, 277.

Parkins, A. S. and Walls, D. F., (1998). Phys. Rep. **303**, 1.

Pedri, P., Pitaevskii, L., Stringari, S., Fort, C., Burger, S., Cataliotti, F. S., Maddaloni, P., Minardi, F., and Inguscio, M., (2001). Phys. Rev. Lett. **87**, 220401.

Phillips, W. D., (1998). Rev. Mod. Phys. **70**, 721.

Pieri, P. and Strinati, G. C., (2000). Phys. Rev. B **61**, 15370.

Pieri, P. and Strinati, G. C., (2003). Phys. Rev. Lett. **91**, 030401.

Pitaevskii, L. P., (1961). Zh. Eksp. Teor. Fiz. **40**, 646. [Sov. Phys. JETP **13**, 451 (1961)].

Raab, E. L., Prentiss, M., Cable, A., Chu, S., and Pritchard, D. E., (1987). Phys. Rev. Lett. **59**, 2631.

Randeria, M., (1995). Crossover from BCS Theory to Bose-Einstein Condensation. In *Bose Einstein Condensation*, edited by Griffin, A., Snoke, D., and Stringari, S., p. 355 (Cambridge University Press, Cambridge, 1995).

Roati, G., Riboli, F., Modugno, G., and Inguscio, M., (2002). Phys. Rev. Lett. **89**, 150403.

Sachdev, S., *Quantum Phase Transitions* (Cambridge University Press, Cambdridge, 1999).

Schmidt, P. O., Hensler, S., Werner, J., Griesmaier, A., Görlitz, A., Pfau, T., and Simoni, A., (2003). Phys. Rev. Lett. **91**, 193201.

Schreck, F., Khaykovich, L., Corwin, K. L., Ferrari, G., Bourdel, T., Cubizolles, J., and Salomon, C., (2001). Phys. Rev. Lett. **87**, 080403.

Schrieffer, J. R., *Theory of Superconductivity* (W. A. Benjamin, New York, 1964).

Sondheimer, E. H. and Wilson, A. H., (1951). Proc. Roy. Soc. A **210**, 173.

Stoddart, J. C., Hilton, D., and March, N. H., (1968). Proc. Roy. Soc. A **304**, 99.

Stringari, S., (1996). Phys. Rev. Lett. **77**, 2360.

Tilley, D. R. and Tilley, J., *Superfluidity and Superconductivity* (Hilger, New York, 1990).

Timmermans, E., Furuya, K., Milonni, P. W., and Kerman, A. K., (2001). Phys. Lett. A **285**, 228.

Treutlein, P., Hommelhoff, P., Steinmetz, T., Hänsch, T., and Reichel, J., (2004). Phys. Rev. Lett. **92**, 203005.

Trombettoni, A. and Smerzi, A., (2001). Phys. Rev. Lett. **86**, 2353.

Truscott, A. G., Strecker, K. E., McAlexander, W. I., Partridge, G. B., and Hulet, R. G., (2001). Science **291**, 2570.

Weinstein, J. D., deCarvalho, R., Guillet, T., Friedrich, B., and Doyle, J. M., (1998). Nature (London) **395**, 148.

Weiss, C. and Eckardt, A., (2004). Europhys. Lett. **68**, 8.

Wierzbowska, M. and Krogh, J. W., (2005). Phys. Rev. B **71**, 014509.

Zwierlein, M. W., Stan, C. A., Schunck, C. H., Raupach, S. M. F., Gupta, S., Hadzibabic, Z., and Ketterle, W., (2003). Phys. Rev. Lett. **91**, 250401.